



© 1995-2026 by Isidoro Martínez

# COMBUSTION KINETICS

Combustion kinetics.....	1
Physical mixing and its effects on ignition, propagation and extinction .....	2
Mixing.....	3
Mixture ratio specification .....	3
Diffusion .....	3
Convection .....	4
Evaporation .....	5
Evaporation from a planar surface .....	6
Droplet evaporation.....	8
Ignition and extinction .....	11
Igniter types.....	13
Propagation of non-premixed flames .....	14
Gas fuel jet .....	15
Flame length.....	15
Condensed fuel.....	16
Flash point (ignition).....	16
Flame stabilisation by porous feeding: oil lamps and the candle flame .....	17
Fuel sprays .....	18
Droplet combustion.....	20
Particle combustion.....	27
Propagation of premixed flames .....	29
Laminar combustion .....	29
Deflagration speed .....	31
Flame thickness.....	33
Flame stabilisation .....	34
Flame quenching .....	35
Flammability limits.....	35
Autoignition temperature .....	37
Supersonic combustion .....	38
Turbulent combustion .....	41
Axisymmetric turbulent jet flames.....	43
Turbulent premixed flames .....	43
Chemical kinetics .....	44
Reaction mechanism and reaction rate.....	44
Mass action law.....	45
Types of elementary reactions .....	46
Arrhenius law .....	47
Collision theory.....	49
Relation between rate coefficients and equilibrium constants.....	50
Kinetics of NO <sub>x</sub> formation .....	51
Catalysis.....	52
The three-way catalytic converter.....	53
Selective catalytic reduction (SCR) .....	53
Catalytic combustion.....	54

## COMBUSTION KINETICS

Thermodynamic laws, establish limits to natural and artificial processes, i.e. bounds to the possible paths, but the path actually followed, and the pace (the process rate), depends on other circumstances. For

instance, Thermodynamics does not say that a piece of paper will burn in air, not even after being ignited, and does not deal with the burning rate; it just says that the system paper/air might reach a more stable equilibrium state (more entropy) by burning, and determines that end state (which might be reached also by secularly-slow oxidation).

It is Kinetics science which deals with how fast things happen: instantly (i.e. more quickly than monitored, as in explosions), evolving at a sizeable pace (i.e. in the monitoring time-span, as in combustion), or at a negligible rate (i.e. more slowly than monitored, as in slow oxidation). For instance, a piece of paper enclosed in a transparent container with more air than the theoretical one, may not burn completely if ignited (e.g. by a concentrated light), because, as oxygen concentration gets reduced, convection and diffusion might not supply enough oxygen to maintain the minimum heat release needed for propagation. Hydrocarbon fuels cannot burn in  $N_2/O_2$  mixtures if  $x_{O_2} < 12\%$  ( $< 5\%$  for  $H_2$  fuel), and hydrocarbon fuels cannot burn in  $CO_2/air$  mixtures if  $x_{O_2} < 15\%$  ( $< 6\%$  for  $H_2$  fuel). At room temperature, without ignition, the piece of paper in air will oxidize very slowly (unnoticeable to the eye).

Topics covered below are: rate of physical mixing and its effects on ignition, propagation and extinction, and rate of chemical reaction once mixed (including a review of reaction mechanisms). Some basic models of global combustors and of flame structure are dealt with apart.

## PHYSICAL MIXING AND ITS EFFECTS ON IGNITION, PROPAGATION AND EXTINCTION

It cannot be stressed enough that kinetics is what finally controls combustion (or any other reaction); Thermodynamics indicates if the reaction is natural (i.e. may proceed in an isolated system) or artificial (i.e. requires some exergy input from outside). Thermodynamics says that a fuel and air may naturally react, but if the kinetics is too slow, an observer concludes that there is no reaction. Some illustrative examples are: the burning of a piece of paper or a candle inside a closed container; the fuel will not burn completely if there is not enough room inside for a good air-convection to the flame, even if with more than stoichiometric air is enclosed.

A vivid example of the controlling effect of mixing is presented in Fig. 1, showing two similar candle flames, one on the ground and the other on a space platform (no buoyancy effects); candle flames on earth are long, slender and yellow, whereas under weightlessness they are nearly spherical, blue, and burn much slower (sometimes get extinguished), due to the lack of air draught by buoyant convection.

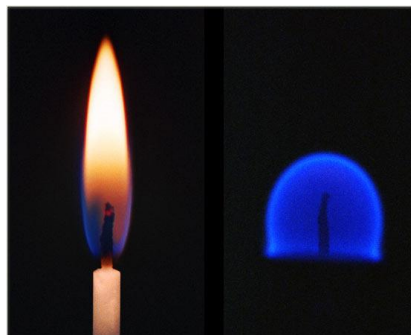


Fig. 1. Candle flames on earth (left) and on a space station under weightlessness (right).

One of the basic features of combustion is its self-spreading power: under usual conditions, a fuel/air mixture, once ignited, generates a flame-front that sustains itself, i.e. that transmits the activation to the fresh mixture through heat and mass transfer. Two limit cases can be considered for this propagation according to the state of the mixture: combustion propagation when fuel and air are at each other side of the flame (i.e. for a non-premixed mixture), and combustion propagation when both fuel and air are at the same side of the flame (i.e. for a premixed flame).

Mass transfer is essential to combustion, which is a special case of combined heat and mass transfer reacting system; and not only inside the combustor itself, but for other combustion-related reactors as in the after-burning catalyts, fuel reformers, etc.

## **MIXING**

Mixing is a pre-requisite for combustion. Mixing (i.e. decreasing bulk differences), is a natural process (i.e. it does not require an energy expenditure), so that, if fuel and oxidizer gases are brought to contact and enough time allowed, a perfect mixing would take place in their energy level (temperature), relative speeds and chemical composition (with the natural stratification in the presence of gravity or another force field).

But mixing is a slow physical process if not forced by convection (large-scale transport) and turbulence (large-scale to small-scale transport). Turbulent mixing is the rule in all practical fluid flows at scales larger than the millimetre, from the piping of water, fuels, gases..., to the wakes behind vehicles of any sort, to all atmosphere, ocean and stellar motions (there are some exceptions, as the laminar diffusing contrails left by jet aircraft)..

Two extreme cases of mixing are considered in combustion: combustion in a premixed system (prepared well-before-hand, or well-stirred), and combustion in the common-interface layer where non-premixed fuel and air come into contact. For premixed combustion, the mixture ratio specification is established before-hand, whereas for non-premixed combustion, the mixture ratio specification depends on the actual feeding flow-rates of fuel and air.

### **Mixture ratio specification**

Mixture ratio specification may use different units: molar fraction of fuel in the mixture  $x_F$ , mass fraction  $y_F$ , fuel-to-air ratio  $f$  (molar or mass), air-to-fuel ratio  $A$  (molar or mass), equivalence ratio  $\phi$  (the actual fuel/air ratio relative to the stoichiometric one, with the same value in molar and mass basis), air relative ratio  $\lambda$  (the air/fuel ratio relative to stoichiometry, with the same value in molar and mass basis), mixture fraction (mass-flow rate ratio of injected fuel to mass flow rate of products), etc.

### **Diffusion**

Actual mixing of chemical species is governed by mass transfer laws, very similar to heat transfer laws for conduction (diffusion) and convection. In a homogeneous media, without phase changes or chemical reactions, the basic kinetic law for mass diffusion is Fick's law:

$$\vec{j}_i = -D_i \nabla \rho_i \quad (\text{Fick's law, similar to Fourier's law for heat transfer } \vec{q} = -k \nabla T) \quad (1)$$

$\vec{j}_i \equiv \dot{m}_i/A$  being the diffusion-mass-flow-rate of species  $i$  per unit area,  $D_i$  the mass-diffusivity for species  $i$  in the given mixture, and  $\rho_i=y_i\rho$  the mass-density of species  $i$  in the given mixture. Notice that only the flux associated to the main driving force is considered in Eq. (1), i.e. mass-diffusion due to a species-concentration gradient; there are also secondary fluxes associated to other possible gradients (e.g. mass-diffusion due to a temperature gradient, known as Soret effect, and mass-diffusion due to a pressure gradient; alternatively, there may be heat-diffusion due to a species-concentration gradient, known as Dufour effect, and heat-diffusion due to a pressure gradient), but most of the times those cross-coupling fluxes are negligible. Besides, selective force fields may yield diffusion (e.g. ions in an electric field).

Notice that only molecular diffusion is considered here, i.e. for particle sizes  $<10^{-8}$  m; particles in the range  $10^{-8}.. 10^{-6}$  m (soot, mist, smoke), are studied with Brownian-motion mechanics, and particles  $>10^{-6}$  m with Newton mechanics.

To better grasp the similarity between species diffusion and heat diffusion, the balance equations for mass-transfer and heat-transfer, applied to a unit-volume system, are here presented jointly:

Magnitude	Accumulation	=	Production	Diffusive flux	Convective flux	
Chemical species $i$	$\frac{\partial y_i}{\partial t}$	=	$\frac{w_i}{\rho}$	$+ D_i \nabla^2 y_i$	$-\nabla \cdot (y_i \vec{v})$	(2)
Thermal energy	$\frac{\partial T}{\partial t}$	=	$\frac{\phi}{\rho c_p}$	$+ a \nabla^2 T$	$-\nabla \cdot (T \vec{v})$	(3)

with  $w_i$  being the mass-production rate by chemical reaction, and  $a=k/(\rho c_p)$  the thermal diffusivity. Notice that there is only one driving heat-transfer-function,  $T$ , but many mass-transfer functions,  $y_i$  (one for each species), although most problems are modelled as a binary system of one species of interest,  $i$ , diffusing within a background mixture of averaged properties. Typical values for  $D_i$  and  $a$  are given in [Mass diffusivity data](#). Because of the nearly-equal values of  $D_i$  and  $a$  for gases ( $D_i \approx a \approx 10^{-5}$  m<sup>2</sup>/s), the thermal and solutal relaxation times in absence of convection, are nearly equal ( $t_{rel} \approx L^2/D_i \approx L^2/a$ ), in spite of the fact that the coefficients in (1) are widely different ( $D_i \approx 10^{-5}$  m<sup>2</sup>/s and  $k \approx 10^{-2}$  W/(m·K)),  $T$  is not bound, and  $\rho_i$  is bound to  $\rho_i \ll 1$  kg/m<sup>3</sup> for diffusion in air under normal conditions. In liquids and solids, mass diffusion relaxation times are much smaller than their thermal counterparts.

## Convection

A quicker mixing process than diffusion is convection, where bulk fluid-flow transports species as if encapsulated, instead of having to migrate by its own random fluctuations.

As in the study of convective heat transfer, the fluid flow should be solved in conjunction to diffusion, but, as in heat transfer, one usually resorts to empirical correlations to compute mass-transfer non-dimensional parameters (Sherwood  $Sh$ , or mass-Nusselt number) in terms of non-dimensional stimuli (e.g. Reynolds number of the imposed flow  $Re$ , Rayleigh number of the imposed thermal gradient  $Ra$ ,

etc.). Thus, instead of solving the whole fluid-dynamic problem with (2-3) and momentum equation, empirical correlations applicable just to the boundary values are often used as:

$$\left. \begin{aligned} Sh &\equiv \frac{h_m L}{D_i} = Sh(Re_L, Sc) \quad \text{for mass convection} \\ Nu &\equiv \frac{hL}{k} = Nu(Re_L, Pr) \quad \text{for heat convection} \end{aligned} \right\} \quad (4)$$

where both, the solutal and thermal convection correlations are sketched ( $Sc \equiv \nu/D_i$ ,  $Pr \equiv \nu/a$ ). Notice, however, that the boundary conditions in practical solutal-convection problems can be very different to the classical heat-convection problems where a single fluid sweeps a hot or cold rigid boundary. The case of a submerged jet is a good case of similarity between solutal convection (e.g. a jet of fuel gas emerging to ambient air) and thermal convection (e.g. a jet of hot air emerging to ambient air).

Phase changing systems are more conspicuous, although most of the times the process of phase change (e.g. the evaporation of liquid fuels studied below) can be separated from the more complex gas-phase combustion. But, in the burning of solid fuels the process are entangled because there may be decomposition reactions within the solid (as in wood burning), or heterogeneous combustion at the interface (as in coal burning and metal burning). For instance, when aluminium particles burn in a carbon-dioxide atmosphere ( $2Al + 3CO_2 \rightarrow Al_2O_3 + 3CO$ ), the initial and final phases take place with a detached vapour flame (at some 2600 K), consuming two thirds of the mass, whereas an intermediate stage takes place at the surface, controlled by a carbon layer (perhaps  $Al_4C_3$ ) formed by heterogeneous reaction of carbon monoxide there (and not by an alumina layer as thought;  $T_m(Al_2O_3) = 2320$  K)..

## EVAPORATION

Evaporation (sometimes called vaporisation) is the net flux of some species, at the interface between a condensed phase and a gas mixture, due to a normal concentration-gradient of that species in the gas close to the interface. Examples: the evaporation of water from a glass of water in air (the level decreases some 1 mm/day); the evaporation of ethanol from a glass of wine in air (water evaporates too); the evaporation of ammonia from an open bottle of water-ammonia solution in air (water evaporates too); the evaporation of naphthalene in air (sometimes called sublimation). Volatiles liquids and volatiles solids are smelly. It is often simpler and more efficient to transport fuels in condensed form, and safer to burn them with non-premixed flames, in which case, fuel droplet evaporation from the injector spray constitutes a first stage to the combustion of the generated vapours within the oxidiser stream (droplet burning is dealt with below; we follow on here just with the evaporation process).

Evaporation should not be confused with boiling (which may also be properly called vaporisation), which is the change of phase within the liquid phase due to an increase in temperature or a decrease in pressure. Perhaps the most clarifying difference is that boiling is a bulk process (bubbles form at hot points, usually the walls of a heated container), and may take place in pure substances, whereas evaporation is a free-surface process (no bubbles form, and the interface region cools) that only happens in mixtures.

Evaporation is a basic topic in combustion of condensed fuels, as well as a more general mass-transfer topic in mechanical engineering (humidification, drying, cooling towers) and chemical engineering (reactors, materials processing, oxidation, electrochemistry, scrubbing, desalination by reverse osmosis and other membrane processes, etc.). Evaporation and condensation in a mixture are always combined mass-and-heat transfer problems (boiling and condensation in a pure substance and the Stefan problem of melting or solidification, are just heat transfer problems).

We only consider here evaporation of a pure liquid, typically water, in air (a mixture), controlled by diffusion of both, species and heat. When considering the vaporisation of practical fuel droplets (like diesel oil), the variation with time of the composition and vaporisation temperature may be very important due to multi-component equilibrium; however, it is common practice in theoretical analysis to assimilate commercial fuels to pure-component reference-fuels, usually n-octane for gasolines, and n-dodecane or n-tetradecane for diesel oils.

### Evaporation from a planar surface

Let us start by the simplest one-dimensional planar diffusion-controlled evaporation problem. Consider a test-tube with water in open air. Assuming that the air in the tube is quiescent, but the air outside is stirred enough as to maintain constant conditions at the mouth ( $T_0, p_0, \phi_0$ ), and assuming a steady state (the water level is thought to be kept steady by some slow liquid supply from the bottom; in the real test-tube case, the liquid level would slowly decrease), Eq. (2) with its initial and boundary conditions would solve the problem, although the first integration can be skipped directly establishing the series of mass conservation relations:

$$\underbrace{\frac{\dot{m}}{A}}_{\text{mass-flow-rate per unit area}} = \rho v = \underbrace{\rho_i (v + v_{diff_i})}_{\text{mass-flow-rate of } i \text{ per unit area}} + \underbrace{0}_{\text{mass-flow-rate of other species per unit area}} = \underbrace{\rho_i v}_{\text{mass of } i \text{ convected}} + \underbrace{j_i}_{\text{mass of } i \text{ diffused}} = \rho_i v - D_i \frac{d\rho_i}{dz} = \underbrace{\rho_{liq} v_{liq}}_{\text{mass-flow-rate of liquid to keep the level steady}} \quad (5)$$

where  $\rho$  is the density of the mixture (assumed constant in a first approximation),  $\rho_i = y_i \rho$ , and  $v_{liq}$  the speed of liquid injection (really, the liquid-level descent with time). Notice that, with the constant-density approximation in the gas phase, the global velocity is also constant along the tube. Dividing by  $\rho$  and integrating, the value of the global velocity is obtained:

$$v = y_i v - D_i \frac{dy_i}{dz} \rightarrow v = -\frac{D_i}{1-y_i} \frac{dy_i}{dz} \rightarrow v = D_i \frac{d \ln(1-y_i)}{dz} \rightarrow v = D_i \frac{\ln \frac{1-y_i}{1-y_{i0}}}{z_1-z_0} \stackrel{y_i \ll 1}{=} -D_i \frac{y_i - y_{i0}}{z_1 - z_0} \quad (6)$$

$y_{i1}$  being the mass-fraction of species  $i$  at the mouth (assumed to be that of the ambient),  $y_{i0}$  the mass-fraction at the bottom of the gas column (i.e. close to the liquid surface), assumed to be that of two-phase equilibrium, i.e. Raoult's law (see [Mixtures](#)), and  $z_1 - z_0$  being the depth (the diffusion length). This result might have been anticipated by a simple dimensional analysis of the function  $v = v(D_i, \Delta y_i, \Delta z)$ .

For water evaporation in ambient air, the mass-fraction of water-vapour,  $y_i$ , at the ambient and at liquid-level equilibrium are related to the pure vapour pressure at that temperature by Raoult's law:

$$y_i = \frac{x_i M_i}{\sum x_i M_i} = x_i \frac{M_i}{M_m} \begin{cases} y_i = \frac{\phi p_i^*(T_{amb})}{p} \frac{M_i}{M_m} & \text{at the ambient} \\ y_{i_0} = \frac{p_i^*(T_{liq})}{p} \frac{M_i}{M_m} & \text{at the liquid surface} \end{cases} \quad (7)$$

where  $M_i$  and  $M_m$  are the molar mass of species  $i$  (the volatile liquid, e.g. water) and the mixture (practically that of ambient air, for small  $x$ 's), respectively, and  $\phi$  is the relative humidity of the ambient. The evaporation speed, (6), with the relation  $\rho v = \rho_{liq} v_{liq}$  from (5), and the linearization in (6) yields:

$$v_{liq} = \frac{\rho v}{\rho_{liq}} = \frac{\rho}{\rho_{liq}} \frac{D_i}{\Delta z} \frac{M_i}{M_m} \left[ \frac{p_i^*(T_{liq})}{p} - \phi \frac{p_i^*(T_{amb})}{p} \right] \quad (8)$$

e.g. the evaporation rate for water at 20 °C in ambient air at 20 °C, 100 kPa and 60% humidity ratio, for a 1 cm diffusion layer, is:

$$v_{liq} = \frac{1.2 \text{ kg/m}^3}{1000 \text{ kg/m}^3} \frac{2.2 \cdot 10^{-5} \text{ m}^2/\text{s}}{1 \cdot 10^{-2} \text{ m}} \frac{0.018 \text{ kg/mol}}{0.029 \text{ kg/mol}} \left[ \frac{2.3 \text{ kPa}}{100 \text{ kPa}} - 0.6 \frac{2.3 \text{ kPa}}{100 \text{ kPa}} \right] = 1.5 \cdot 10^{-8} \text{ m/s} \quad (1.3 \text{ mm/day})$$

where  $D_i$  was found from [Mass diffusivity data](#), and the vapour-pressure value obtained from [steam tables](#) (or from Clapeyron equation, or [Antoine fitting](#)). Notice that the evaporation rate increases with vapour pressure (e.g. ethanol evaporates some 10 times faster than water at 20 °C  $v_{liq}=12$  mm/day), whereas for a less volatile fuel like n-decane it is <0.1 mm/day), and it falls with deepness (e.g. 0.13 mm/day for water down 10 cm in a test-tube).

It was J. Dalton in 1801, just after he introduced the partial-pressure concept, who first said that the evaporation rate is proportional to the difference in partial pressure of water vapour from the saturated boundary layer, to that of the air far aside, and that it increases with free air velocity. The first analytical model of evaporation is due to J. Stefan in 1872. The effect of wind speed is to decrease the boundary layer thickness, directly related to the diffusion depth,  $\Delta z$ , we have assumed known, consequently increasing the evaporation rate.

Evaporation not only implies a mass transfer but also a heat transfer, since the vaporization enthalpy at the liquid surface must come from either the liquid side or the air side, at the steady state. This heat-transfer implication was not apparent in the numerical application of (8) just done, because the two temperatures were assumed known, but in reality, the temperature at the liquid interface will depend on the heat transfer and energy balance (the effect of a possible radiation trapping there, e.g. from sun rays, will enter here also); for a small amount of liquid the liquid quasi-steady temperature would be the wet-bulb temperature (see [Humid air](#)), a little below ambient temperature, making the approximation above acceptable.

The analysis of evaporation in very hot environments (e.g. inside a furnace), gets more involved. To start with, Raoult's law is no longer applicable to the far field ( $r \rightarrow \infty$ ) because the liquid could not be in two-phase equilibrium with such a hot gas (i.e.  $T_\infty > T_{cr}$ , or at least  $p^*(T_\infty) > p$ ), although they are still applicable at the liquid surface because the droplet tends to reach a quasi-steady-state temperature close to its boiling point. Besides, the linearisation in (6) may no longer be valid, and the large temperature and concentration variation makes the constant-property assumption less accurate.

### Droplet evaporation

Evaporation of a droplet in a quiescent atmosphere is a more practical application of this diffusion-controlled model, since small drops (say of 1..10  $\mu\text{m}$ ), as found in mists and spray combustion, quickly accommodate their speed to that of the surrounding gas flow, suppressing forced-convection effects afterwards; besides, natural convection effects, due to buoyancy of the lighter humid mixture nearby, is neglected in this analysis. Convection would increase the evaporation rate, of course.

Consider the system defined by the control volume enclosed by a generic sphere of radius  $r > r_0$ ,  $r_0$  being the radius of the droplet, kept steady by an imaginary supply of liquid at the origin (in reality, the droplet radius will decrease with time since there is not such an imaginary supply). The expected radial profiles for the mass fraction and temperature fields are presented in Fig. 2.

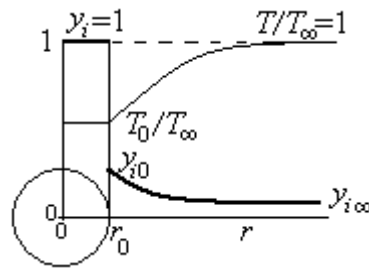


Fig. 2. Radial profiles of temperature and mass fraction of the volatile component, in a droplet evaporation process.

The mass and energy balance for this strictly-steady system (with a liquid source at  $r=0$  and a vapour sink at  $r=\infty$ ), can be set as follows:

Magnitude	Accumulation	Production	Diffusive flux	Convective flux
Mass balance (global)	0	= $\dot{m}_L$	+0	$-\dot{m}(r)$ (9)
Mass balance (volatile species)	0	= $\dot{m}_L$	$+AD_i \frac{d\rho_i}{dr}$	$-\dot{m}(r)y_i$ (10)
Energy balance	0	= $-\dot{m}_L h_{LV_0}$	$+Ak \frac{dT}{dr}$	$-\dot{m}(r)c_{p_i}(T-T_0)$ (11)

where the enthalpy reference has been chosen  $h=0$  for the vapour,  $i$ , at the liquid temperature  $T_0$  (that is why a  $-h_{LV,0}$  input at the origin is accounted for in (11)). Notice that the thermal capacity in the convective flux must be the vapour one, because the sum  $\sum \rho_i v_i c_{p_i} A$  reduces to just the vapour term  $\rho_i v_i c_{p_i} A$  (because dry air cannot move in the steady state), and  $\rho_i v_i A = \rho v A = \dot{m}$ .

In (9),  $\dot{m}_L$  stands for the mass-flow-rate of liquid consumed (the parameter sought), and one concludes that the global mass-flow-rate of gases across the spherical surface,  $\dot{m}(r)$ , is independent of  $r$ , and, from  $\dot{m} = \rho v A$ , the bulk radial velocity  $v$ , assuming constant gas density  $\rho$  (pressure is constant and temperature does not vary too much), and with  $A=4\pi r^2$ , finally yields:

$$\dot{m} = \rho v A = \text{constant} \longrightarrow v(r) = \frac{v_0 r_0^2}{r^2} \quad (12)$$

Dividing (10) by  $\dot{m}_L = \rho v A$  and upon integration, yields:

$$\begin{aligned} 0 &= 1 + \frac{D_i}{v} \frac{dy_i}{dr} - y_i \longrightarrow 0 = 1 + \frac{r^2 D_i}{v_0 r_0^2} \frac{dy_i}{dr} - y_i \Rightarrow \frac{D_i}{v_0 r_0^2} \frac{dy_i}{1 - y_i} = d \frac{1}{r} \Rightarrow \\ v_0 &= \frac{D_i}{r_0} \ln \frac{1 - y_{i,0}}{1 - y_{i,\infty}} = -\frac{\rho_{liq}}{\rho} \frac{dr_0}{dt} \Rightarrow \frac{dr_0^2}{dt} = -\frac{2\rho D_i}{\rho_{liq}} \ln \frac{1 - y_{i,0}}{1 - y_{i,\infty}} \equiv -K \Rightarrow t_{evap} = \frac{r_{0,ini}^2}{K} \end{aligned} \quad (13)$$

i.e. the well-known Langmuir's law (1918), or simply the  $r^2$ -law, stating that the droplet life-time,  $t_{evap}$ , is proportional to the square of the initial radius; often, the diameter,  $d$ , is used instead of radius (with our  $K$ ,  $d^2(t) = d_0^2 - 4Kt$ ).

There is, however, an internal unknown in (13),  $y_{i,0}$ , which is controlled by the energy balance (11): the heat for the liquid-to-vapour transition must come from the gas phase (droplets always attain a quasi-steady temperature below that of the environment, even if injected hotter); evaporation always implies a coupled heat and mass transfer.

Dividing now the energy balance (11) by  $\dot{m}_L = \rho v A$  and upon integration yields:

$$\begin{aligned} 0 &= -h_{LV_0} + \frac{k}{\rho v} \frac{dT}{dr} - c_{p_i} (T - T_0) \Rightarrow \frac{dT}{h_{LV_0} + c_{p_i} (T - T_0)} = -\frac{\rho v}{k} dr = -\frac{\rho v_0 r_0^2}{k r^2} dr \Rightarrow \\ \ln \frac{h_{LV_0} + c_{p_i} (T_\infty - T_0)}{h_{LV_0}} &= \frac{c_{p_i} \rho v_0 r_0}{k} = -\frac{c_{p_i} \rho_{liq}}{k} \frac{dr_0}{dt} r_0 \Rightarrow \frac{dr_0^2}{dt} = -\frac{2k}{\rho_{liq} c_{p_i}} \ln \frac{h_{LV_0} + c_{p_i} (T_\infty - T_0)}{h_{LV_0}} \\ \Rightarrow t_{evap} &= \frac{r_{0,ini}^2}{\frac{2k}{\rho_{liq} c_{p_i}} \ln \left( 1 + \frac{c_{p_i} (T_\infty - T_0)}{h_{LV_0}} \right)} = \frac{r_{0,ini}^2}{\frac{2\rho D_i}{\rho_{liq}} \ln \frac{1 - y_{i,0}(T_0)}{1 - y_{i,\infty}}} \end{aligned} \quad (14)$$

where the latter equality comes from (13), and is the closure for the evaporation problem, relating mass diffusion and heat diffusion, and having only one unknown  $T_0$  after imposing Raoult's law (7):  $y_{i,0}(T_0) = (p_i^*(T_0)/p)(M_i/M_m)$ .

For instance, if a 0.1 mm in diameter water-droplet is injected in air at 1000 °C, the droplet-temperature quickly (in less than 1 ms) adapts to a temperature of 63 °C, evaporating in some 0.17 s. The initial

relative motion decays also quickly (in some 10 ms). The vapour-mass-fraction close to the droplet is not 'near 1' as one might guess from such a 'burning' environment, but a mere 16% (notice that the air surrounding the drop is just about 63 °C and not 1000 °C). As another example, the evaporation time for a 10 µm n-decane droplet issuing at 400 K (50 °C below its boiling point) into air preheated to 800 K in a furnace, is some  $1.2 \cdot 10^{-3}$  s. Fuel droplets are usually assumed to evaporate in a zero-fuel environment, i.e. into 'dry air' but, sometimes, the surrounding atmosphere may already contain some fuel vapours from the evaporation of surrounding droplets in a spray.

As in the planar-geometry evaporation case treated above, convection effects in droplet evaporation can be neglected in the species balance (10) and in the energy balance (11), but not in the overall mass balance (9), if the gas is not too hot (let say for  $T_\infty < 100$  °C), what is equivalent to linearising the logarithms in (14), reducing to:

$$\Rightarrow t_{\text{evap}} = \frac{r_{0,\text{ini}}^2}{\frac{2k}{\rho_{\text{liq}}} \frac{(T_\infty - T_0)}{h_{LV_0}}} = \frac{r_{0,\text{ini}}^2}{\frac{2\rho D_i (y_{i,0}(T_0) - y_{i,\infty})}{\rho_{\text{liq}}}} \quad (15)$$

which, together with  $y_{i,0}(T_0) = (p_i^*(T_0)/p)(M_i/M_m)$ , allow the finding of  $T_0$ ,  $y_{i,0}$ , and  $t_{\text{evap}}$ .

It can be shown that, for room-temperature water droplets,  $T_0$  is the wet-bulb temperature, practically coinciding with the adiabatic-saturation temperature analysed in [Humid air](#) and easily found with the psychrometric chart, or analytically by an enthalpy matching. For instance, a water droplet 0.1 mm in diameter in ambient air at 25 °C, 100 kPa and 50%RH, attains a temperature of  $T_{\text{wet bulb}} = 17.6$  °C, and evaporates in some 16 s.

Notice that the choice of system for the analysis can be changed, and, instead of the spherical volume of radius  $r > r_0$ , used above to establish the mass and energy balances (9-11), a unit area in a spherical surface of radius  $r > r_0$  could have been used, and typical Fluid Mechanics formulation applied:

$$\frac{D(\sum \rho_i e_i)}{Dt} + \nabla \cdot (\rho_i h_i \vec{v}_i) = -\nabla \cdot \vec{q} \longrightarrow 0 + \rho_v c_{p_v} \frac{dT}{dr} v_r = \frac{k}{r^2} \frac{d}{dr} \left( r^2 \frac{dT}{dr} \right) \quad (16)$$

which, after performing a first integration from  $r_0$  to  $r$ , knowing from the mass balances (9) that  $\rho v_r = \rho_0 v_0 = \rho_0 r_0^2 / r^2$ , would yield a similar equation to (11):

$$\rho v_0 \frac{r_0^2}{r^2} c_{p_v} \frac{dT}{dr} = \frac{k}{r^2} \frac{d}{dr} \left( r^2 \frac{dT}{dr} \right) \longrightarrow \rho v_0 r_0^2 c_{p_v} (T - T_0) = k r^2 \frac{dT}{dr} - \rho v_0 r_0^2 h_{lv_0} \quad (17)$$

where the last term comes from the energy balance at the surface,  $\dot{m} h_{lv_0} = 4\pi r_0^2 k \frac{dT}{dr} \Big|_{r=r_0}$ . A second integration would yield:

$$\frac{dT}{h_{lv_0} + c_{p_v}(T - T_0)} = \frac{\rho v_0 r_0^2}{k} \frac{dr}{r^2} \rightarrow \ln \left( \frac{h_{lv_0} + c_{p_v}(T_\infty - T_0)}{h_{lv_0}} \right) = \frac{\rho v_0 r_0 c_{p_v}}{k} = \frac{\rho_{liq} v_{liq} r_0 c_{p_v}}{k} \quad (18)$$

and so on as from (14).

## IGNITION AND EXTINCTION

We shall deal basically with steady-state kinetics and propagation, but sooner or later, as for most engineering problems, besides analysing the steady running, one has to face the more complex phenomena of starting up and stopping down the process (ignition and extinction), not only to better understand combustion, but to provide a practical control of fire.

Ignition of a reactive system may be homogeneous (only for perfectly premixed systems uniformly heated, as in compression ignition), or heterogeneous, as when locally initiated by a spark or a catalyst in either a premixed or a non-premixed system (a subsequent deflagration front, i.e. a flame, develops).

All combustion reactions have positive affinities and thus could proceed naturally in an isolated system, but most common fuels and oxidisers combine too slowly at ambient conditions, if an activation energy is not externally supplied, i.e. an ignition source, like an electric spark or a hot object, to cause a self-acceleration of the reaction. After ignition, the reaction self-propagates because a flame is an ignition source, as any other hot object.

One may consider different ways for the fuel/oxidiser reaction to run away:

- Contact ignition, i.e. by just coming into contact some special fuels with special oxidisers (ignition by contact with a hot object is covered under autoignition). There are substances (called pyrophoric substances) which have autoignition temperatures below that of the environment (say <15 °C), so that the combustion takes place as soon as they are put in contact (they cannot exist premixed). At room conditions, the mixture of hydrogen and fluorine, H<sub>2</sub>(g)/F<sub>2</sub>(g), burns without an ignition source; the mixture H<sub>2</sub>(g)/Cl<sub>2</sub>(g) does not burn by contact in the dark, but intense light, or the presence of Pt, Pd or Ni ignites it. Dimethyl-hydrazine (N<sub>2</sub>H<sub>2</sub>(CH<sub>3</sub>)<sub>2</sub>(l)) and dinitrogen tetroxide (N<sub>2</sub>O<sub>4</sub>(g)) also burn just by contact, and the mixture H<sub>2</sub>(g)/O<sub>2</sub>(g) also burns at room conditions by contact in the presence of platinum catalyst. Even in normal air there may be spontaneous combustion of some fuels, as when phosphine bubbles, obtained by immersion of phosphorous in a sodium hydroxide solution, P<sub>4</sub>(s)+3NaOH(aq)+3H<sub>2</sub>O(l)=PH<sub>3</sub>(g)+3NaH<sub>2</sub>PO<sub>2</sub>(aq), escapes at the free surface and react with air, PH<sub>3</sub>(g)+2O<sub>2</sub>(g)=(1/4)P<sub>4</sub>O<sub>10</sub>(s)+(3/2)H<sub>2</sub>O(g). Also, when a solution of white phosphorus in carbon disulfide is used to write on paper, the carbon disulfide evaporates within a few minutes and the paper chars. Pure iron in minute amounts also burn by contact with air (this is how sparks are produced when hitting a piece of iron on a flint). Although not properly a combustion process, the rapid exothermic oxidation of metallic sodium in contact with water, Na(s)+H<sub>2</sub>O(l)=Na(OH(aq)+(1/2)H<sub>2</sub>(g), may release so much energy as to ignite the hydrogen produced. There have been accidents where oil-impregnated rags have got fire by themselves because of the rapid oxidation of oil in air with such a large contact area and low heat transfer.

- Spark ignition, i.e. by locally supplying the activation energy required to triggers the reaction, based on the production of a tiny burning particle (e.g. by striking a piece of flint and steel together) as in prehistoric times, or on the electric arc produced between two closed electrodes when the dielectric strength of the medium is surpassed (3 kV/mm for air). The latter is a very convenient ignition method, used in Otto engines, gas turbines, furnaces and boilers, but requires a premixture at least locally near the spark plug (see Flash point, below). An order-of-magnitude estimation of the energy required for ignition is the energy required to heat a cubic volume of size  $L_{th}$  to the autoignition temperature, i.e.,  $\Delta E_{ign} \sim L_{th}^3 \rho c_p \Delta T_{ign} \sim (10^{-3})^3 \cdot 1 \cdot 10^3 \cdot 10^3 \sim 10^{-3}$  J, as mentioned above. It is estimated that the spark produces a plasma filament at some 20 000 K in the discharge, quickly turning into a hot gas-ball of one or two millimetres in diameter at some 5000 K, from which the normal deflagration theory applies. The spark plug was invented by N. Tesla in 1890 (also attributed to R. Bosh and to K. Benz).
- Autoignition, usually by compression ignition, but also by hot-surface ignition, i.e. by raising the temperature of the gases by rapid compression or by heat transfer, either previously mixed, or, more commonly, by raising the temperature of the oxidiser in a sudden compression and then injecting the fuel when desired and at the desired rate. This is a very convenient ignition method, which may be applied to the non-premixed mixture as in the usual Diesel engine (i.e. to ignite a cold liquid jet being injected in hot surrounding air), or to a fully premixed mixture (as in some new stationary Diesel engines where all the fuel is injected before ignition takes place by compression), or to a dual-fuel Diesel engines (as when a lean natural gas / air mixture is premixed and made to ignite by compression-ignition of a low-autoignition secondary fuel pilot injection). Autoignition by hot spot is usually an undesirable event, only used purposely in minute model engines.
- Catalytic ignition. By using a catalyst to lower the activation energy. For instance, a  $H_2(g)/O_2(g)$  mixture within a glass or a steel bottle at room temperature and pressure is not seen to react (hardly any molecule yield fertile chocks, releasing negligible heat); the effect of a sizeable spark ( $>1$  mJ) in a sizeable container (larger than a few millimetres by all sides), a hard knock, or the presence of a sizeable amount of platinum, is required to ignite the system at ambient conditions (it may also be ignited by heating the mixture to 850 K at 100 kPa whatever the container).

Combustion ignition in reciprocating engines must be stimulated at each cycle (either by a spark or by quick compression), but in steady combustors like gas turbines, furnaces and boilers, the system only needs to be ignited at start of the duty (usually by spark plugs); although sometimes a pilot flame is maintained if operation is discontinuous (e.g. in some domestic hot-water heaters).

Once ignited, for a flame to propagate, a certain balance between the heat released (depending on chemical kinetics) and heat transfer towards the fresh mixture, must be warranted, what explains the existence of flammability limits and quenching distance (explained below), as well as the process of ignition and extinction themselves.

Combustion may be difficult to start, but it may be more difficult to stop. Besides the obvious extinction procedure of letting all the fuel to burn (the amount of oxidiser is assumed infinite in terrestrial

applications), and avoiding any more fuel to be near the flame, a combustion process may be arrested by providing unfavourable conditions to its propagation, namely, by cooling and/or by dilution of its reactive species (fuel, oxidiser, and the many radicals needed for flame propagation).

The traditional fire-fighting method of massively adding water, works mainly as a cooling agent to lower the temperature below the autoignition value, to prevent flame propagation, whereas the typical CO<sub>2</sub> fire-extinguisher works mainly as a dilutant to prevent air coming into the flame (see [Fire safety](#)).

Cold solid walls, with their massive thermal sinks, also act as cooling agents that prevent flame propagation near them; safety lamps and quenching grids are based on that fact. For instance, premixed methane/air combustion cannot propagate inside a metal tube of less than 2 mm bore. This value corresponds to the quenching distance for stoichiometric mixtures; for lean and rich mixtures the quenching distance grows parabolically towards infinite at the ignition limits (e.g. for methane/air, it goes from 1.8 mm at  $\lambda=1$ , to 4 mm at  $\lambda=0.8$  and  $\lambda=1.8$ ).

Many types of igniters have been developed. A summary of ignition devices, classified by the ignition method, follows.

### Igniter types

- Thermal
  - Rapid-compression heating
    - Air-compression igniter, as in a diesel engine; some primitive people knocked in a crude piston-cylinder device to ignite some dry wood-shavings inside.
  - Spark heating
    - The flint-and steel spark. Usually, a gripping steel wheel is force to rotate a little against a small flint stone, and iron sparks are projected over some easily flammable substance: LPG (since 1933), gasoline vapour (since 1932) or waxy wool (tinder, since prehistoric times). Little sensitive to moisture.
    - Two-electrode sparks. Electric discharge through a  $\sim 1$  mm air-gap (requires a coil autotransformer to overcome rupture voltage in gases, i.e.  $>3$  kV/mm), on use since 1850. Sensitive to moisture.
    - Piezoelectric sparks. Created when some natural crystalline substances (quartz, barium titanate) are hammered (a mechanical trigger is used), causing opposite electrical charges to concentrate on each side of the crystal. Non-sensitive to moisture.
    - Electronic sparks. Since 1980. All lighters until 1990 where of non-premixed type, but since then, induction-type premixed flames, nearly invisible and much more powerful, are produced in 'jet lighters' (miniature bunsens).
  - Dissipative heating
    - Mechanical energy dissipation. The bow and drill is the most-efficient simple-friction fire-making procedure since prehistoric times. Very sensitive to moisture.
    - Electrical energy dissipation. A battery and a wire or a steel-wool load that gets red-hot by Joule heating. Sometimes the wire is a catalyst (see below).

- Pyrotechnic heating
  - [The match](#). It is the most handy igniter since XIX c. With a little friction, a specially prepared chemical substance quickly reacts and forms a flame. Sensitive to moisture.
- Radiation heating
  - Solar radiation and a glass magnifier (water-filled bottles, or even a clear ice ball) focussing light onto tinder. Non-sensitive to moisture.
  - Pulse laser can be focused on the most convenient spot; the combination of pulse-mode semi-conductor lasers and optical fibres seem most promising. Non-sensitive to moisture.
- Pure chemical (without heating)
  - Simple contact of special chemicals (e.g. hydrogen with fluoride).
  - Catalytic igniter. Platinum wire gets red-hot, reaching  $>1000$  K, when in contact with an hydrogen/air mixture. sustaining combustion even of other combustible mixtures. For propane and butane flames, the catalytic wire is usually preheated electrically. This device is used in modern, wind-proof lighters, producing a steady blow-torch type of flame nearly-invisible in the bright (sometimes a ceramic flame-window that glows when hot is used to indicate the lighter is on).

In spite of all the above possibilities, to be successful in using an igniter to start a camp fire, as important as the lighter, is to get ready dry flammable tinder (fine wood shavings, dried grass, straw, down from corn or from birds or seeds, etc.).

Ignition is a requisite for combustion, but fire-keeping demands also self-sustained conditions for its propagation (very easily obtained with flammable material, but sometimes not so easy with other combustible material).

## PROPAGATION OF NON-PREMIXED FLAMES

Non-premixed flames (also *diffusion* flames, but all flame requires diffusion) are established by some ignition process (usually by a spark or by high temperature of the oxidiser), near the boundary between fuel and oxidiser, not having a defined propagation speed and flammability limits as premixed flames. The main characteristic of a non-premixed flame is its size and shape.

Non-premixed flames may be laminar (e.g. candle flame, droplet burning) or turbulent (e.g. open fires), and they are quite luminous (yellow, because of blackbody emission by soot) except for hydrogen flames, that are nearly invisible (alcohol flames are difficult to see, too).

Burke and Schumann established in 1928 the first model of non-premixed flames (coaxial flows with the same speed), based on the assumption that the characteristic chemical time for reaction is much shorter than the time required for the reactives to reach the flame (mixing time), what implies very fast kinetics and very thin flame thickness. The fluid field is split by the flame in a fuel-region with no oxidiser ( $y_O=0$ ), and an oxidiser-region with no fuel ( $y_F=0$ ; i.e.  $y_F y_O=0$  in the whole field), the flame sitting just where the two reactive flows meet with stoichiometric rates (i.e. for a reaction  $F + \nu_O O \rightarrow \nu_P P$ , where  $\rho_O \vec{v}_O / M_O + \nu_O \rho_F \vec{v}_F / M_F = 0$ ); besides, if chemical kinetics is so fast that the global process is diffusion-

controlled, both  $y_F=0$  and  $y_O=0$  at the flame front. This Burke and Schumann's model of fast chemical kinetics is the first step in most analysis of non-premixed combustion.

Non-premixed flames are most used in practical system (coal burning, gas-fired or oil-fired industrial burners, diesel engines, gas turbines, and solid-fuel rockets), because of their higher safety and ease of control, in spite of being less power-intensive and more pollutant than premixed combustion. They are easier to establish than premixed flames, as everybody lighting a bunsen realises, because they naturally hold attached to the injector rim over a very wide regime range, and they are more radiant, what is an advantage for old lighting-methods and long-range heating. Unsteady non-premixed flames occur in diesel engines.

To ignite a non-premixed fuel/oxidiser mixture, some ignition agent must be applied at the mixing layer (outside this fluid interface, the fluid is not flammable because only fuel or oxidiser exist). The usual way to ignite this local premixture is by an electrical spark or a pilot flame, but auto-ignition at high temperature is used in diesel engines. Detailed studies in simple configurations, like the autoignition of a small fuel droplet in hot air (well above the autoignition temperature), shows that ignition takes place (after some delay time) in the lean and hotter zone sited some 10 droplet-radius afar (with relative air/fuel ratios  $\lambda=2.5..3$ ). The square-law for droplet-diameter evolution,  $d^2(t)=d_0^2-Kt$ , applies very well to both the non-reacting evaporation and to the combustion processes, with typical values of  $K$  heavily dependent on temperature ( $K=10^{-7}..10^{-6}$  m<sup>2</sup>/s in droplet combustion in cold or hot air).

## GAS FUEL JET

### Flame length

Flame length is the most characteristic parameter of a non-premixed flame established at the mouth of an injector; the most common example may be the flame of a cigarette lighter. Flame length depends on the measuring principle: visible light, other radiations, temperature field, concentration fields, and the averaging principle for fluctuating flames. It also depends on buoyancy; e.g. propane/air jet flames issuing from a 0.8 mm tube, linearly increase their height with exit velocity up to 12 m/s ( $Re \approx 1000$ ), with heights of 0.25 m for buoyant flames (on the ground) and 0.33 m for non-buoyant flames (under microgravity). Further increasing of exit velocity causes a transition to turbulent flames with heights receding to 0.18 m for buoyant flames, until they blow out at 33 m/s, whereas for non-buoyant flames heights further increase to 0.39 m, until some 35 m/s, when they shorten to some 0.29 m before blow out at 40 m/s. Notice that, at high speeds, buoyancy should not be as relevant as it appears in practice (perhaps the behaviour would tend to match, if blow-out did not prevent it).

A quick guess for the laminar flame length,  $L_{fl}$ , may be given by the distance travelled by the jet at the exit speed  $w_0$  during the period of fuel diffusion  $t_{dif}$ , from  $y_F=1$  at the jet centre, to the stoichiometric value  $y_F=y_{F,stoq}$  at the flame front; i.e.  $L_{fl}=t_{dif}w_0$ , with  $t_{dif}=(1-y_{F,stoq})(D_0/2)^2/D_i$  and thence:

$$L_{fl}=(1-y_{F,stoq})w_0D_0^2/(4D_i). \quad (19)$$

For instance, for the propane/air jet-flame above-mentioned, at  $w_0=12$  m/s, with  $D_0=0.8$  mm,  $D_i=10^{-5}$  m<sup>2</sup>/s and  $y_{F,stoq}=1/(1+16)=0.06$ , we get  $L_{fl}=0.18$  m, against the 0.25 m measured.

Notice that with this model (only applicable to laminar jet flames,  $Re<1000$ ) the flame length is proportional to the volumetric flow-rate, and increases with stoichiometric air/fuel ratio (e.g. carbon-monoxide flame are much shorter than hydrocarbon flames,  $L_{CO}/L_{CH4}\approx 0.2$ ,  $L_{H2}/L_{CH4}\approx 0.2$ ,  $L_{C4H10}/L_{CH4}\approx 3$ ). Turbulent non-premixed flames flicker with a wide frequency spectra, but the main first natural frequency,  $f_n$ , decreases with size in the form  $f_n \approx f_0 / \sqrt{D/D_0}$ , with  $f_0=1.5$  Hz and  $D_0=1$  m,  $D$  being the diameter of the fuel-injection tube or the mean horizontal size for open fires (it seems that this is due to the Kelvin-Helmholtz vortex-ring instability in the shear layer of the hot plume, outside the flame).

Non-premixed flames may radiate a lot of energy. For gas-jet flames of a few kilowatts issuing from a few-millimetre injector, from 10% (for methane/air) to 50% (for propane/air) of their heat release is lost by radiation, mainly by blackbody emission at some 2500 K, from the in-flame soot (with a smooth maximum at  $C_{Wien}/T=2900/2500=1.2$   $\mu\text{m}$ , but with a more pronounced peak between 4  $\mu\text{m}$  and 5  $\mu\text{m}$  due to molecular band emission by H<sub>2</sub>O and CO<sub>2</sub>).

Similarly to the temperature field, soot production in a gas-fuel jet flame, concentrates in the mixing shell where the flame locates at small heights, and wide-spreads to the centre downstream (e.g. for a steady methane jet of 10 mm diameter issuing in air at 80 mm/s, soot volume fractions profiles have a two-bell shape up to some 50 mm height, and one central bell-shape further along the axis).

In most practical non-premixed burners, air is coaxially fed with the fuel, what may increase the flame length and pollutant emissions if the co-flow pattern reduces the mixing. To prevent this, special swirl-inducing nozzles are used to quickly mix fuel and air, greatly reducing flame length.

## CONDENSED FUEL

### Flash point (ignition)

Another aspect related to the combustion of non-premixed mixtures is the so called ‘flash point’ of a condensed fuel in the presence of ambient air. In the limit case of the initial liquid fuel before evaporation (i.e. no fuel-vapours in the air), combustion is not possible, but, as soon as evaporation proceeds, a gaseous fuel/air mixture develops near the liquid surface, with a fuel-vapour mole fraction that may be below the lower flammability limit (see Flammability limits, below), in between the lower and upper flammability limits, or above the upper limit. Of course, all this depends on temperature, since vapour pressure exponentially grows with temperature.

The flash point is the lowest temperature at which a liquid has a sufficient vapour pressure to ignite when a small pilot flame is brought close to the surface of the liquid. Table 1 shows some flash point data (more can be found [aside](#)).

Table 1. Flash-point temperature for liquid fuels in air at 100 kPa.

Fuel	$T_{\text{flash}}$
------	--------------------

Methane	−188 °C	85 K
n-Butane	−63 °C	210 K
Iso-Octane	−12 °C	261 K
n-Heptane	−4 °C	269 K
Methanol	12 °C	285 K
Ethanol	12 °C	285 K
n-Octane	13 °C	286 K
n-Decane	44 °C	317 K
Diesel	50 °C	323 K
Kerosene	57 °C	330 K
n-Dodecane	71 °C	344 K
Lubrication oil	200 °C	500 K

Liquids (and solids) with flash points below 40 °C (or 50 °C, the flash point for diesel; the choice is arbitrary and depends on legislation) are labelled ‘flammable’, and above that are labelled ‘combustible’. Many common organic-liquid solvents have a flash point below room temperature, posing a great fire hazard: e.g. benzene (−11 °C), acetone (−18 °C), diethyl ether (−45 °C). Some of them will maintain their flammability risk even at concentrations as low as 10% by weight in water; e.g. isopropanol and ethanol have flash points below the threshold of 38 °C at concentrations as low as 30% by weight in water. A pool of light fuel oil with a flash point above 60 °C cannot be ignited with a match.

Crude-oil is easy to ignite because of its many volatiles, requiring extensive safety measures for its handling and transport, but crude-oil spills at sea cannot be ignited because volatiles swiftly go away and heavies cannot be heated enough because of the large thermal sink of underlying water (oil spills have to be cleaned mechanically and with chemical solvents).

The state of the fuel sample (particularly for solid fuels), its humidity, the composition of the oxidising atmosphere, or finely dividing the fuel (sprays and powders), can significantly change the flash point. Sprays of pure fuel show lower flash points, but sprays of diluted fuels (e.g. alcohol/water mixtures) show higher flash points. Wood shaving ignites more readily than a massive piece of wood.

### **Flame stabilisation by porous feeding: oil lamps and the candle flame**

Condensed fuels can be ignited by a spark if they are above their flash-point temperature (at least locally); if not, they have to be heated before ignition starts, perhaps just holding close a match for a while, providing the heating and the igniter at the same time. Once ignited, the non-premixed flame will travel along the fuel surface, usually becoming unstable, and even extinguishing by poor ventilation (lack of air). All these problems are solved when the flame can get stabilised around the tip of a porous solid that pumps liquid-fuel by capillary suction towards a well-ventilated region, what is the foundation of oil lamps and candles; a torch being a hybrid device between a candle and an oil lamp (a torch is a wooden or tow shaft dipped in wax, tallow or pitch, and set alight by an igniter). Some oil lamps developed in the 19th century used gravity-pumping instead of capillary pumping. A detailed description of the historical developments of oil lamps (where the fuel is already in the liquid state), and of candles (where the fuel is in the solid state, but a local molten pool is maintained by heat radiation from the flame), can be found aside, in [History of Fuels. Torches, oil lamps and candles](#)).

The length of this type of flames depends to some extent on the length of the wick, what can be controlled in oil lamps (too long wicks will burn themselves if unable to pump enough liquid). The structure of a typical candle flame is depicted in Fig. 3. Initially, the wick holds some solid wax in its pores (from previous use or from manufacturing). The wax can be of animal origin (esters of fatty acids, like stearin and beeswax) or of mineral origin (long-chain paraffins, beyond eicosane,  $C_{20}H_{42}$ ,  $T_m=36.4\text{ }^\circ\text{C}$ ). When a match is brought nearby, first the wax melts (between  $50\text{ }^\circ\text{C}$  and  $60\text{ }^\circ\text{C}$ ), then the vapours heat up to the flash point (around  $230\text{ }^\circ\text{C}$ , i.e.  $600\text{ K}$ ), ignition starts, and a quasi-steady-state regime is reached; a 20 mm in diameter candle burns some 5..10 g/h of fuel, yielding some 60..120 W ( $LHV_{\text{wax}}=44\text{ MJ/kg}$ ), with a flame height of 40..45 mm in still air, and a maximum flame diameter of some 8..10 mm.

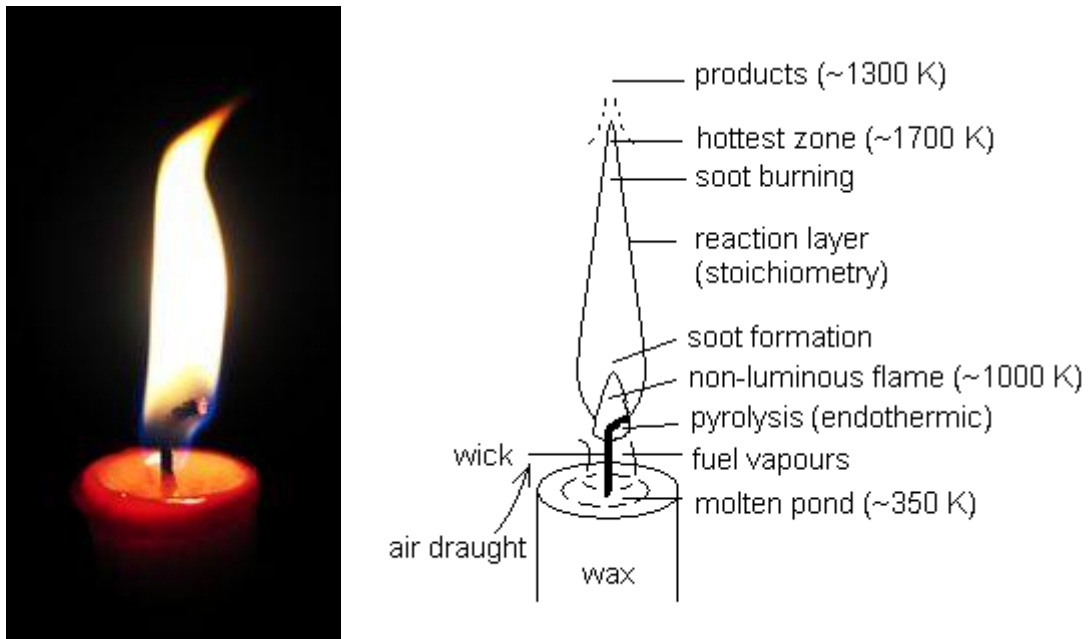


Fig. 3. Mixing processes and structure of a candle flame.

These flames radiate a lot of energy, and, although most of this low-temperature blackbody-radiation is in the infrared spectrum, the small visible part more than justified their prominent use for artificial lighting since prehistoric times, until the development of electric light at the end of the 19th century.

A typical candle flame has a colour temperature of some 1700 K, what is responsible for the typical yellow colour of non-premixed flames. A volume fraction of soot less than 1 ppm already gives luminous blackbody emission. This is similar to the incandescent radiation from a filament electrically heated to near 3000 K as in the traditional incandescent bulb-lamp (white light corresponds to the solar spectrum, nearly a perfect blackbody at 5800 K). Soot formation is a relatively slow chemical process of nucleation and aggregation, and it is enhanced by increasing the residence time within the flame and by the presence of polycyclic aromatic hydrocarbons (PAH), so that, when flickering occurs in turbulent flames, soot production quickly rise.

### Fuel sprays

Because of the advantage of easy storage and high energy intensity, liquid fuels are used in the majority of vehicle-engines (cars, trucks, trains, ships, and aircraft), and in a sizeable part of stationary engines and power plants. The combustion is performed by injection of the liquid fuel in an oxidiser gas stream

(usually air), and it is of utmost importance for a good burning to promote the interface area between liquid and gas, where, in most cases, a non-premixed flame will be established; the exception is when the injected liquid can be left to fully evaporate and a subsequent premixed flame produced, as in gasoline engines.

The scattering of the injected liquid into fine droplets (spray, or atomisation; see Fig. 4), is usually achieved mechanically by creating a high-speed jet ( $>100$  m/s, what requires very high pressure jumps, currently up to 200 MPa in some diesel injectors), which disintegrate into droplets (much smaller than the jet diameter), by shear forces. Think about how fast the processes follow each other: in a few milliseconds, a thin liquid stream in turbulent motion (which may cavitate and flash-boil when approaching the tip of the fuel injector), forms a spray that breaks down to a myriad of [droplets, which evaporate, ignite, burn](#), and generate unwanted [emissions](#). Wall impingement is undesirable in most circumstances, increasing emissions by poor combustion near cold walls; even in gasoline injection at the manifold, wetted surfaces introduce an undesirable time-lag in the fuel control loop.

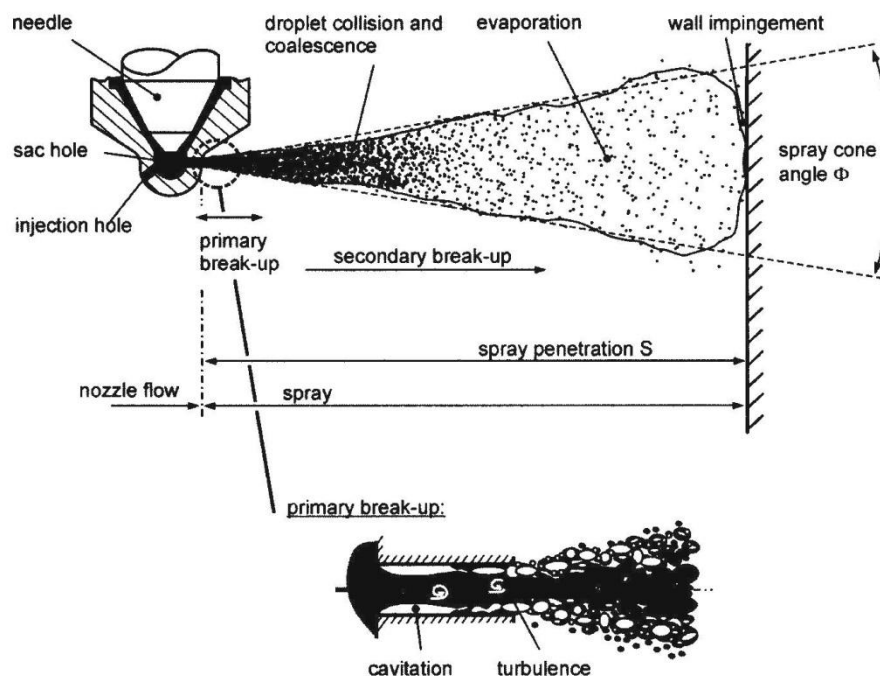


Fig. 4. Jet break-up, droplet formation and evaporation in a diesel injector.

The break-up length, i.e. the length where the first droplets appear (at the jet surface), tends to zero in atomised jets (Fig. 5). Other methods of spraying, as impinging jets, air-entrained or water-entrained jets, are less used in combustion.

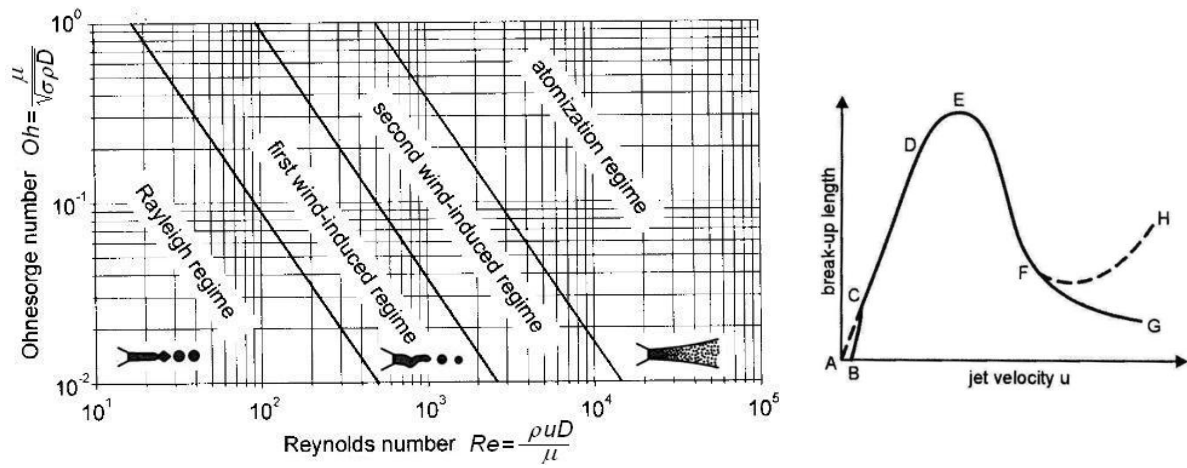


Fig. 5. Liquid-jet break-up regimes in terms of Reynolds number  $Re \equiv \rho u D / \mu$ , and Ohnesorge number  $Oh \equiv \mu / (\sigma \rho D)^{1/2}$ . For a given injector diameter  $D$ , and given liquid (of density  $\rho$ , viscosity  $\mu$ , and surface tension  $\sigma$ ), the only variable is injection speed  $u$ . In the Rayleigh regime, drops larger than the jet diameter are cast by capillary instability, and the break-up length grows proportionally to the speed (A to D). In the first wind-induced regime, droplet size decreases to the range of jet diameter, and the break-up length decreases too (E to F), but still being much larger than the diameter. In the second wind-induced regime, droplet size further decreases, and break-up length tends to zero (F to G, at the surface; there is a longer liquid spike at the core that grows with speed, F to H). The atomization regime stands beyond this zero-break-up-length point (beyond G).

Steady non-premixed flames occur in liquid-fired gas turbines, boilers and furnaces, whereas unsteady non-premixed flames occur in diesel engines. Typically, a jet of liquid fuel is injected (at some 350 K once warmed by the hot engine), inside hot air (heated to some 950 K by adiabatic compression). Due to the fine atomisation achieved by the high pressure injector, a cloud of fuel vapour, well-mixed with air, develops around the liquid jet already after a few millimetres from the injector; at a distance of a few centimetres, this rich vapour mixture already attains its autoignition temperature (the minimum for diesel/air is 480 K, but up to 800 K are measured before proper ignition), pyrolyses and burns, attaining more than 2500 K and showing chemiluminescent radiation; beyond that, soot starts to form at the tip of the jet due to thermal pyrolysis of air-depleted vapours, and soot formation continues until there is liquid remaining.

In the dual-fuel diesel engine, a lean mixture of air / natural gas is usually formed in the admission manifold, and, once compressed to the normal compression ratio of the diesel engine, is ignited by a injection of a small amount of diesel oil at the usual high pressure near the top dead centre; the temperature increase during compression of the mixture is high enough to auto-ignite the oil (480 K for diesel/air) but not enough to auto-ignite the gaseous mixture (850 K for methane/air), helped also by the larger autoignition delay of methane than that of diesel oil.

Notice that LPG injection, and heated gasoline and diesel injection, can give rise to flash-boiling (i.e. if the injection enthalpy is higher than the saturated-liquid enthalpy at the discharge pressure), with a very effective atomisation. Presently, it is only of interest in gasoline injectors in the intake manifold.

### Droplet combustion

A single droplet of fuel burning in air, is not of any practical use (except for research), but it is of paramount importance for the understanding of spray combustion, a very practical arrangement used in all

liquid-fuel burners, all diesel engines, and kerosene gas-turbines. The key parameter to be found is the droplet burning time, what governs the path length before burnout (and consequently the minimum size of the combustion chamber required), and the required residence time for unsteady processes (and consequently the minimum period in reciprocating engines).

We here assume that the combustion has already been started, either by a spark in cold air (above the flash-point temperature), or by autoignition in hot air (above autoignition temperature). Pressure, assumed constant during droplet combustion, has an influence on several aspects of the droplet-burning process, including flame dynamics, combustion chemistry, evaporation rate, heat-up period, and ignition delay time. For instance, droplet combustion experiments show that, after ignition, the flame increases in size initially by thermal expansion and internal convection, but later decreases in size, following the shrinking of the droplet (but not linearly proportional as deduced below with a simple model).

To further simplify the single-droplet problem, we assume it to be spherically-symmetric (a good approximation under microgravity, because, on Earth, a vertical plume develops; by the way, microgravity also allows easy droplet positioning by levitation). Additionally, we focus just on the quasi-steady rate of burning, after the initial processes of ignition (heating, species diffusion, and reaction activation) had been settled. As for droplet evaporation, we can imagine a liquid source at the centre of the drop to keep a strict steady state. In this steady-rate regime, sketched in Fig. 6, the droplet temperature keeps a constant value  $T_0$  (a heat-and-mass diffusion trade-off value to be found, lower than its boiling point), with heat from the flame diffusing inwards and forcing evaporation, which supplies fuel vapours with a mass fraction  $y_{F0}$  close to the liquid, diffusing outwards and feeding a non-premixed flame, located at  $r_1/r_0 \approx 10$ , fed also from the outside by a diffusive flow of oxygen from the air, with both fuel and oxidiser concentrations approaching zero at the flame (with slopes proportional to the stoichiometry). Products being generated at the flame (we assume the single-step reaction model  $F + \nu_O O \rightarrow \nu_P P$ ), and part of the heat released, diffuse outwards. A possible inert gas, notably nitrogen for combustion in air, completes the set of species playing (one must have at every point  $y_F + y_O + y_P + y_N = 1$ ).

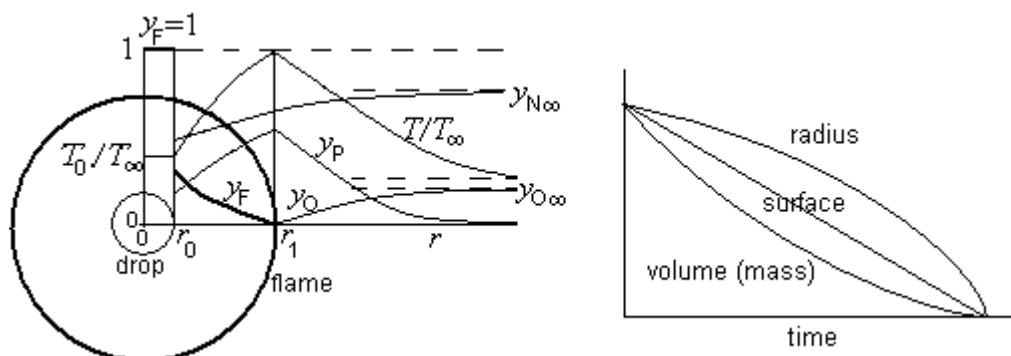


Fig. 6. Droplet combustion. a) Temperature and species-concentration profiles (combustion in air). b) Evolution of drop radius, area, and volume, with time.

We start the analysis of droplet combustion by rewriting the equations for droplet evaporation (9-11), i.e., the global mass balance, species mass balance, and energy balance, for a spherical volume of radius  $r$  (now it must be  $r_0 < r < r_1$ ), with  $y_F + y_P + y_N = 1$  and only the fuel flowing (from the source at the origin, to the sink at the flame; there is no sink for  $y_P$  or  $y_N$  at  $r_0$ ):

Magnitude	Accumulation	Production	Diffusive flux	Convective flux	
Mass balance (global)	0	= $\dot{m}_F$	+0	$-\dot{m}(r)$	(20)
Mass balance of fuel (volatile species)	0	= $\dot{m}_F$	$+AD_F\rho\frac{dy_F}{dr}$	$-\dot{m}(r)y_F$	(21)
Energy balance	0	= $-\dot{m}_F h_{LV_0}$	$+Ak\frac{dT}{dr}$	$-\dot{m}(r)c_{pF}(T-T_0)$	(22)

These equations must be now supplemented with the mass diffusion balances for the other species (all minus one, if we make use of the global balance). To simplify nomenclature, we make use of the stoichiometric relation,  $F + \nu_O O \rightarrow \nu_P P$ , from the start. The choice of system for analysis is always a control volume of radius  $r$  in strict steady state (with appropriate sources and sinks at discontinuities). For the oxidiser, we must choose a sphere with  $r > r_1$  (there is no oxidiser in  $r < r_1$ ). The oxidiser has a source at  $r \rightarrow \infty$  and a sink at the flame (at  $r = r_1$ ), of algebraic amount  $-\dot{m}_O$  related to the fuel flow-rate by the stoichiometry at the flame:  $\dot{m}_O/M_O = \nu_O \dot{m}_F/M_F$ ; notice that the stoichiometric coefficients  $\nu_i$  are in molar basis (that is why the molar masses appear in the mass-equations).

Magnitude	Accumulation	Production	Diffusive flux	Convective flux	
Mass balance of oxidiser ( $r > r_1$ )	0	= $-\dot{m}_F \nu_O \frac{M_O}{M_F}$	$+AD_O\rho\frac{dy_O}{dr}$	$-\dot{m}(r)y_O$	(23)
Mass balance of products ( $r > r_1$ )	0	= $\dot{m}_F \nu_P \frac{M_P}{M_F}$	$+AD_P\rho\frac{dy_P}{dr}$	$-\dot{m}(r)y_P$	(24)
Mass balance of products ( $r < r_1$ )	0	= 0	$+AD_P\rho\frac{dy_P}{dr}$	$-\dot{m}(r)y_P$	(25)
Mass balance of nitrogen (any $r$ )	0	= 0	$+AD_O\rho\frac{dy_O}{dr}$	$-\dot{m}(r)y_O$	(26)

the latter being redundant since at any stage we have  $y_F + y_O + y_P + y_N = 1$ .

The overall mass balance (20) is still valid for any  $r$ , on either side of the flame, since there are sources and sinks of species at the flame front, but total mass is conserved. Thus, the global mass-flow-rate of gases across any spherical surface,  $\dot{m}(r)$ , is independent of  $r$ , and the bulk radial velocity  $v$ , assuming constant gas density  $\rho$  (no as good an approximation as for the droplet evaporation case studied before, since, although pressure is also assumed constant, temperature varies a lot in droplet combustion), yields:

$$\dot{m} = \rho v A = \text{constant} = \dot{m}_F \longrightarrow v(r) = \frac{v_0 r_0^2}{r^2} \quad (27)$$

The convective speed in the gas phase close to the drop,  $v_0$ , relates to the radius recession rate in the real process through the mass conservation at the liquid surface:

$$\rho v A = \rho v_0 A_0 = \rho_{liq} \left( -\frac{dr_0}{dt} \right) A_0 \longrightarrow v_0 = -\frac{\rho_{liq}}{\rho} \frac{dr_0}{dt} \quad (28)$$

The species balance of fuel in  $r_0 < r < r_1$ , equation (21), divided by  $\dot{m}_F = \rho v A$  and upon integration, yields:

$$\begin{aligned} 0 &= 1 + \frac{D_F}{v} \frac{dy_F}{dr} - y_F \Rightarrow 0 = 1 + \frac{r^2 D_F}{v_0 r_0^2} \frac{dy_F}{dr} - y_F \Rightarrow \frac{D_F}{v_0 r_0^2} \frac{dy_F}{1 - y_F} = d \frac{1}{r} \Rightarrow \\ &\Rightarrow \frac{D_F}{v_0 r_0^2} \ln(1 - y_{F,0}) = \frac{1}{r_0} - \frac{1}{r_1} \end{aligned} \quad (29)$$

The species balance of oxidiser in  $r_1 < r < \infty$ , equation (23), divided by  $\dot{m}_F = \rho v A$  and upon integration, yields:

$$\begin{aligned} 0 &= -v_0 \frac{M_O}{M_F} + \frac{D_O}{v} \frac{dy_O}{dr} - y_O \Rightarrow 0 = -v_0 \frac{M_O}{M_F} + \frac{r^2 D_O}{v_0 r_0^2} \frac{dy_O}{dr} - y_O \Rightarrow \frac{D_O}{v_0 r_0^2} \frac{dy_O}{v_0 \frac{M_O}{M_F} + y_O} = -d \frac{1}{r} \Rightarrow \\ &\Rightarrow \frac{D_O}{v_0 r_0^2} \ln \frac{v_0 \frac{M_O}{M_F} + y_{O,\infty}}{v_0 \frac{M_O}{M_F}} = \frac{1}{r_1} \end{aligned} \quad (30)$$

The energy balance in  $r_0 < r < r_1$ , equation (22), divided by  $\dot{m}_F = \rho v A$  and upon integration yields:

$$\begin{aligned} 0 &= -h_{LV_0} + \frac{k}{\rho v} \frac{dT}{dr} - c_p (T - T_0) \Rightarrow \frac{dT}{h_{LV_0} + c_p (T - T_0)} = -\frac{\rho v}{k} dr = -\frac{\rho v_0 r_0^2}{k r^2} dr = \frac{\rho v_0 r_0^2}{k} d \frac{1}{r} \Rightarrow \\ \ln \frac{h_{LV_0} + c_p (T_1 - T_0)}{h_{LV_0}} &= \frac{c_p \rho v_0 r_0^2}{k} \left( \frac{1}{r_0} - \frac{1}{r_1} \right) \square \frac{c_p \rho v_0 r_0}{k} = -\frac{c_p \rho_{liq}}{k} \frac{dr_0}{dt} r_0 \Rightarrow \\ &\Rightarrow \frac{dr_0^2}{dt} = -\frac{2k}{\rho_{liq} c_p} \ln \left( 1 + \frac{c_p (T_1 - T_0)}{h_{LV_0}} \right) \equiv -K \Rightarrow t_{burn} = \frac{r_{0,ini}^2}{K} \end{aligned} \quad (31)$$

i.e. getting the well-known  $r^2$ -law (similar to Langmuir's law (1918) for droplet evaporation), stating that the droplet life-time,  $t_{burn}$ , is proportional to the square of the initial radius; often, the diameter,  $d$ , is used instead of radius (with our  $K$ ,  $d^2(t) = d_0^2 - 4Kt$ ). The first derivation of this burning time was done by Spalding and Godsave in 1953. Notice that this constant  $K$  for the burning problem will differ in value from that of the simple evaporation problem.

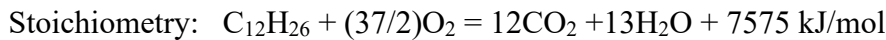
If the steady-state temperature of the drop,  $T_0$ , and its corresponding vaporisation enthalpy,  $h_{LV_0}$ , are approximated by the boiling-point values ( $T_b$  and  $h_{LV_b}$ , or any other suitable value, because the influence on (31) is not large), the energy balance gives directly the burning rate; afterwards, the species balances can be used to get the actual droplet temperature and other internal unknowns, as fuel-mass-fraction near the liquid surface, and products-mass-fractions.

The simplification introduced along (31),  $1/r_1 \ll 1/r_0$ , is justified by practical results ( $r_1/r_0 \geq 10$ ). Later, the flame position  $r_1$  will be found from (27), but the droplet life-time is directly given by the integrated energy equation (28) because we know the flame temperature  $T_1$ , which is the adiabatic flame temperature,  $T_{ad}$ , (we neglect radiation losses) given by:

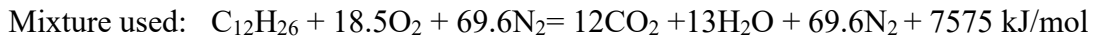
$$T_1 = T_{ad} = T^\oplus + \frac{\text{LHV}_{\text{molar}}}{\sum_{\text{prod}} \nu_i c_{p,i}} \quad (32)$$

where  $\text{LHV}_{\text{molar}}$  stands for the lower heating value of the fuel in molar basis,  $T^\oplus=298$  K is the standard reference in Thermochemistry,  $\nu_i$  are the molar coefficients of the products (including any possible inert species), and  $c_{p,i}$  their molar thermal capacities. One can make the approximation of considering just one thermal-capacity value for the products mixture,  $c_p$ , usually that of air at some appropriate conditions intermediate between the extreme temperatures; the values  $c_p=34$  J/(mol·K)=1200 J/(kg·K) may be used for combustion in air (care is needed, however, to account for the mol-ratio or the mass-ratio of products, including inerts, relative to the fuel. As a rule of thumb, an order-of-magnitude value for the adiabatic temperature of  $T_{ad}=2500$  K may be used for a first approximation.

In summary, for a given fuel droplet in a given environment, data are: initial droplet radius (e.g.  $r_{0,\text{ini}}=10^{-5}$  m), ambient air temperature, pressure and oxygen concentration (e.g.  $T_\infty=300$  K,  $p=100$  kPa,  $y_{O_\infty}=0.23$ ), thermal properties of ambient air (for the given state,  $c_p=1000$  J/(kg·K),  $\lambda=0.024$  W/(m·K), and  $M_O=0.029$  kg/mol), properties of fuel (e.g. for n-dodecane, a pure-substance model for diesel oil (a commercial distillate),  $\rho_{\text{liq}}=780$  kg/m<sup>3</sup>,  $T_b=489$  K,  $h_{\text{LVb}}=257$  kJ/kg,  $M_F=0.170$  kg/mol,  $\nu_O=37/2=18.5$ ,  $\nu_P=12+13=25$ ,  $\text{LHV}_{\text{mass}}=45$  MJ/kg, and  $T_{ad}=2600$  K), the latter obtained from the thermochemical analysis:



the latter obtained from  $\text{LHV}_{\text{molar}} = -\sum \nu_i h_{f,i} = -[-12(-393.52) - 13(-241.82) + (-291)] = 7575$  kJ/mol and thence  $\text{LHV}_{\text{mass}} = 7.575/0.170 = 44.6$  MJ/kg. The actual mixture used in the case of burning in air is:



and consequently:

$$T_1 = T_{ad} = T^\oplus + \frac{\text{LHV}_{\text{molar}}}{\sum_{\text{prod}} \nu_i c_{p,i}} = 298 + \frac{7575 \cdot 10^3}{(12 + 13 + 69.6) \cdot 34} = 2650 \text{ K}$$

or, in mass terms:

$$T_1 = T_{ad} = T^\oplus + \frac{\text{LHV}_{\text{mass}}}{\frac{m_{\text{prod}}}{m_{\text{fuel}}} c_p} = 298 + \frac{44.6 \cdot 10^3}{\frac{0.170 + 18.5 \cdot 0.032 + 69.6 \cdot 0.028}{0.170} \cdot 1200} = 2630 \text{ K}$$

From the energy balance (31) we get the burning time:

$$t_{\text{burn}} = \frac{r_{0,\text{ini}}^2}{K}, \quad \text{with} \quad K = \frac{2k}{\rho_{\text{liq}} c_p} \ln \left( 1 + \frac{c_p (T_1 - T_0)}{h_{LV_0}} \right) \square \frac{2k}{\rho_{\text{liq}} c_p} \ln \left( 1 + \frac{c_p (T_1 - T_b)}{h_{LV_b}} \right) =$$

$$= \frac{2 \cdot 0.024}{780 \cdot 1200} \ln \left( 1 + \frac{1200(2650 - 489)}{257 \cdot 10^3} \right) = 0.12 \cdot 10^{-6} \frac{\text{m}^2}{\text{s}} \Rightarrow t_{\text{burn}} = \frac{r_{0,\text{ini}}^2}{K} = \frac{(10^{-5})^2}{0.12 \cdot 10^{-6}} = 0.83 \cdot 10^{-3} \text{ s}$$

i.e., a  $r_{0,\text{ini}} = 10 \mu\text{m}$  n-dodecane droplet burns in 0.8 ms (typical uncertainties are  $\pm 20\%$ ). Associated to the burning rate in terms of radius (31) is the burning rate in terms of fuel mass:

$$\dot{m}_F = -4\pi r_0^2 \frac{dr_0}{dt} = 2\pi r_0 K = 2\pi K \sqrt{r_{0,\text{ini}}^2 - Kt} \Rightarrow \dot{m}_{F,\text{ini}} = 2\pi r_{0,\text{ini}} K = 2\pi \cdot 0.003 \cdot 0.12 \cdot 10^{-6} = 2.3 \cdot 10^{-9} \text{ kg/s}$$

The flame radius,  $r_1$ , (relative to the drop radius,  $r_0$ ) can be obtained from the oxidiser mass balance (23):

$$\frac{D_{\text{O}_2}}{v_0 r_0^2} \ln \frac{v_0 \frac{M_{\text{O}_2}}{M_F} + y_{\text{O}_2,\infty}}{v_0 \frac{M_{\text{O}_2}}{M_F}} = \frac{1}{r_1} \xrightarrow{v_0 = -\frac{\rho_{\text{liq}}}{\rho} \frac{dr_0}{dt}} \frac{r_1}{r_0} = \frac{\rho_{\text{liq}}}{\rho} \frac{\frac{1}{2} \frac{dr_0^2}{dt}}{D_{\text{O}_2} \ln \left( 1 + \frac{y_{\text{O}_2,\infty}}{v_0 \frac{M_{\text{O}_2}}{M_F}} \right)} \stackrel{\frac{k}{\rho c_p} \approx D_{\text{O}_2}}{=} \frac{\ln \left( 1 + \frac{c_p (T_1 - T_0)}{h_{LV_0}} \right)}{\ln \left( 1 + \frac{y_{\text{O}_2,\infty}}{v_0 \frac{M_{\text{O}_2}}{M_F}} \right)}$$

the latter obtained by substituting the burning-rate result (31) and introducing the approximation of equal thermal and solutal diffusivities in the gas phase (Schmidt number unity). With our example data:

$$\frac{r_1}{r_0} = \frac{\ln \left( 1 + \frac{c_p (T_1 - T_0)}{h_{LV_0}} \right)}{\ln \left( 1 + \frac{y_{\text{O}_2,\infty}}{v_0 \frac{M_{\text{O}_2}}{M_F}} \right)} = \frac{\ln \left( 1 + \frac{1200(2650 - 489)}{257 \cdot 10^3} \right)}{\ln \left( 1 + \frac{0.23}{\frac{15}{2} \frac{0.032}{0.170}} \right)} = \frac{\ln(1+10)}{\ln(1+0.066)} = 37$$

i.e. the flame stabilises itself at a distance of some 37 radii from the drop (of course, with an uncertainty proportional to the simplifications assumed).

The mass fraction of fuel vapours close to the drop, can be computed from the fuel mass balance (21). Proceeding as before, we get:

$$\frac{D_F}{v_0 r_0^2} \ln(1 - y_{F,0}) = \frac{1}{r_0} \xrightarrow{v_0 = -\frac{\rho_{\text{liq}}}{\rho} \frac{dr_0}{dt}} \ln(1 - y_{F,0}) = -\frac{\rho_{\text{liq}}}{\rho} \frac{\frac{1}{2} \frac{dr_0^2}{dt}}{D_F} \stackrel{\frac{k}{\rho c_p} \approx D_{\text{O}_2}}{=} -\ln \left( 1 + \frac{c_p (T_1 - T_0)}{h_{LV_0}} \right) \Rightarrow$$

$$(1 - y_{F,0}) \left( 1 + \frac{c_p (T_1 - T_0)}{h_{LV_0}} \right) = 1 \Rightarrow y_{F,0} = \frac{1}{1 + \frac{h_{LV_0}}{c_p (T_1 - T_0)}} = \frac{1}{1 + \frac{257 \cdot 10^3}{1200(2650 - 489)}} = \frac{1}{1 + \frac{1}{10}} = 0.91$$

i.e., there is some 91% in mass of fuel vapours close to the drop (the uncertainty may be large).

The mass fraction of products,  $y_P$ , in the outer region can be computed from the products mass balance for  $r > r_1$  (24), similarly to that of oxidiser, but now with  $y_{P,\infty} \rightarrow 0$ , what yields:

$$0 = v_P \frac{M_P}{M_F} + \frac{D_P}{v} \frac{dy_P}{dr} - y_P \longrightarrow \frac{D_P}{v_0 r_0^2} \ln \frac{v_P \frac{M_P}{M_F}}{v_P \frac{M_P}{M_F} - y_{P,1}} = \frac{1}{r_1} \longrightarrow \frac{r_1}{r_0} = \frac{\ln \left( 1 + \frac{c_p (T_1 - T_0)}{h_{LV_0}} \right)}{\ln \left( \frac{v_P \frac{M_P}{M_F}}{v_P \frac{M_P}{M_F} - y_{P,1}} \right)} \Rightarrow$$

$$\Rightarrow \frac{\ln \left( 1 + \frac{1200(2650 - 489)}{257 \cdot 10^3} \right)}{\ln \left( \frac{25 \frac{0.030}{0.170}}{25 \frac{0.030}{0.170} - y_{P,1}} \right)} = 37 \Rightarrow y_{P,1} = 0.35$$

i.e., at the flame,  $y_{P,1} = 0.35$ , and, since there is neither fuel nor oxidiser at the flame radius (see Burke-Schuman's model, above), the rest must be inert component,  $y_{N,1} = 0.65$ . In the inner region the equation is (25), what yields:

$$0 = 0 + \frac{D_P}{v} \frac{dy_O}{dr} - y_P \longrightarrow \frac{D_P}{v_0 r_0^2} \ln \frac{y_{P,1}}{y_{P,0}} = \frac{1}{r_1} \longrightarrow \frac{r_1}{r_0} = \frac{\ln \left( 1 + \frac{c_p (T_1 - T_0)}{h_{LV_0}} \right)}{\ln \left( \frac{y_{P,1}}{y_{P,0}} \right)} \Rightarrow$$

$$\Rightarrow \frac{\ln \left( 1 + \frac{1200(2650 - 489)}{257 \cdot 10^3} \right)}{\ln \left( \frac{0.35}{y_{P,0}} \right)} = 37 \Rightarrow y_{P,0} = 0.03$$

i.e., close to the drop,  $r = r_0$ , the composition is  $\{y_{F,0}, y_{O,0}, y_{P,0}, y_{N,0}\} = \{0.91, 0, 0.03, 0.06\}$ , at the flame,  $r = r_1$ , the composition is  $\{y_{F,0}, y_{O,0}, y_{P,0}, y_{N,0}\} = \{0, 0, 0.35, 0.65\}$ , and at  $r \rightarrow \infty$   $\{y_{F,0}, y_{O,0}, y_{P,0}, y_{N,0}\} = \{0, 0.23, 0, 0.77\}$ . The last development could have been applied to the inert component, what yields the relation  $y_{N,1}/y_{N,0} = y_{P,1}/y_{P,0}$ . As for the composition profiles along  $r$ , equations (29-31) should not be integrated between the limits, but up to a generic  $r$ , what yields exponential profiles for all the variations, as sketched in Fig. 6.

## Particle combustion

We consider here the combustion of solid particles, liquid particles being considered above under Droplet combustion. The main differences to the latter are:

- Particles shape can depart a lot from the spherical shape, because there are no surface tension effects as in droplets. Fine solid particles, however, are usually the result of a milling process that tends to produce not too-elongated particles.
- In the case of metallic particles, the combustion products are usually solid oxides (even at the high-temperatures involved).
- Inert solid material (ash) may be a sizeable part of solid fuel (e.g. in some coals), leaving a porous solid layer around the burning fuel core, significantly distorting mass and heat transfer.
- Contrary to liquids, the combustion of solids can take place at the interface (heterogeneous combustion). This is because liquids cannot get hot enough to sustain a rapid surface-oxidation process with the adsorbed oxidiser; they vaporise before. But solids can indeed get very hot and yield a sizeable rate of chemical recombination at their surface layer. For a reaction scheme  $F + \nu_O O \rightarrow \nu_P P$ , fuel and oxidiser flow-rates still must verify  $\rho_O \bar{v}_O / M_O + \nu_O \rho_F \bar{v}_F / M_F = 0$  at the reaction front, but now there are discontinuities in the species concentration at the front, with  $y_F = 1$  and  $y_O = 0$  in the solid phase, and  $y_F = 0$  and  $y_O > 0$  in the gas phase, the oxidiser concentration decreasing towards zero as temperature increase.
- Under some circumstances, two combustion fronts may develop: the heterogeneous one at the particle surface mentioned above, and a homogeneous detached flame as in droplet burning.
- Solid particles are far more difficult to ignite than droplets (they have higher flash points).

Ignition and combustion of pulverized coal particles is of major interest to modern coal-fuelled power plants. Combustion of metal powders and polymeric dust in air is a major safety concern in many powder industries (e.g. flour in food processing, saw-dust in wood processing).

The nature of coal combustion depends a lot on composition and temperature. Leaving aside coal composition (see [Coal analysis, in Fuel properties](#)), the effect of temperature on pure-carbon combustion is as follows (temperature range is very sensitive to humidity):

- For  $T_0 < 1500$  K, i.e. when the surface temperatures (after ignition) does not go over 1500 K, a heterogeneous combustion process is established at the surface according to  $C + O_2 \rightarrow CO_2$ .
- For  $1500 \text{ K} < T_0 < 2500$  K, a heterogeneous endothermic reaction sets at the surface, according to  $C + CO_2 \rightarrow 2CO$ , driven by a gas-phase homogeneous combustion with a blue free flame at some distance from the surface, according to  $CO + (1/2)O_2 \rightarrow CO_2$ .
- For  $2500 \text{ K} < T_0 < 3500$  K, the external free-flame disappears, leaving just the heterogeneous combustion at the surface according to  $C + (1/2)O_2 \rightarrow CO$ .
- For  $T_0 > 3500$  K, evaporation is so effective (carbon sublimates at 3910 K at 100 kPa) that a detached flame develops as in droplet combustion, according to  $C + (1/2)O_2 \rightarrow CO$ , although oxygen dissociation becomes important too.

The surface temperature in carbon combustion depends on how quick heterogeneous reactions proceed relative to the species-diffusion rates, what depends on geometry, trace contaminants, catalysts, etc. In the

simplest case of diffusion-limited combustion at low ambient temperatures, once the heterogeneous reaction  $C+O_2 \rightarrow CO_2$  is established, a surface temperature is in the range  $1000\text{ K} < T_0 < 1500\text{ K}$  is obtained, with a radial profiles as sketched in Fig. 7a, whereas for higher temperatures,  $1500\text{ K} < T_0 < 2500\text{ K}$ , a detached flame appears, with a radial profiles as sketched in Fig. 7c.

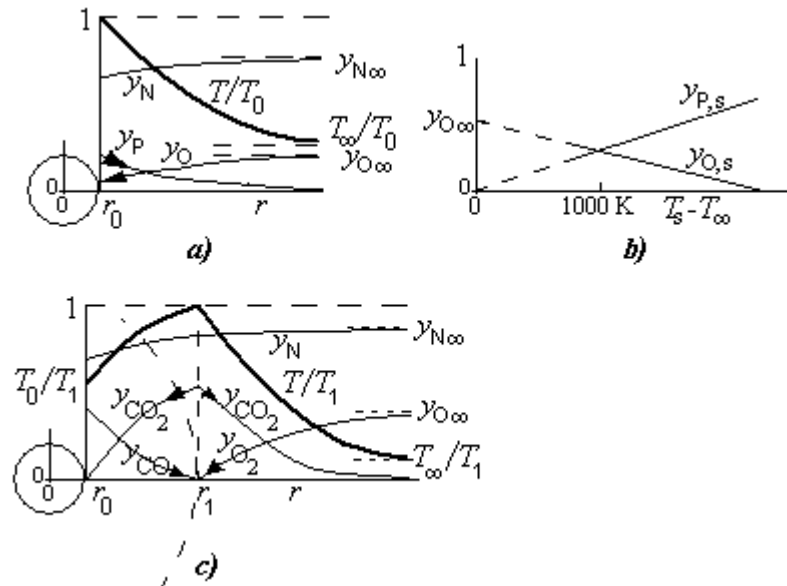


Fig. 7. Combustion of a carbon particle: a) Radial temperature and species concentration profiles when  $1000\text{ K} < T_0 < 1500\text{ K}$  (the only product, P, is CO); b) Correlation of species concentration close to the surface, with surface temperature, for  $1000\text{ K} < T_0 < 1500\text{ K}$ ; c) Radial temperature and species concentration profiles when a detached flame appears ( $1500\text{ K} < T_0 < 2500\text{ K}$ ).

The species and energy balances for the case without free flame, closely following the analysis detailed above for droplet burning, yield:

$$\left\{ \begin{array}{l} \frac{dr_0^2}{dt} = -K = -\frac{2\rho D_O}{\rho_{sol}} \ln \left( \frac{v_O \frac{M_O}{M_F} + y_{O,\infty}}{v_O \frac{M_O}{M_F} + y_{O,0}} \right) \square - \frac{2\rho D_O}{\rho_{sol}} \frac{y_{O,\infty} - y_{O,0}}{v_O \frac{M_O}{M_F}} \\ \frac{dr_0^2}{dt} = -K = -\frac{2\rho D_P}{\rho_{sol}} \ln \left( \frac{v_P \frac{M_P}{M_F}}{v_P \frac{M_P}{M_F} - y_{P,0}} \right) \square - \frac{2\rho D_P}{\rho_{sol}} \frac{y_{P,0}}{v_O \frac{M_O}{M_F}} \\ \frac{dr_0^2}{dt} = -K = -\frac{2k}{c_p \rho_{sol}} \ln \left( \frac{HV + c_p (T_\infty - T^\oplus)}{HV + c_p (T_0 - T^\oplus)} \right) \square - \frac{2k}{c_p \rho_{sol}} \frac{c_p (T_\infty - T_0)}{HV} \end{array} \right. \quad (33)$$

what relates all other variables with the surface temperature attained; e.g., assuming  $D_O = D_P = k/(\rho c_p)$ , with  $HV = 33\text{ MJ/kg}$  for  $C+O_2 \rightarrow CO_2$ , and  $c_p = 1200\text{ J/(kg/K)}$ , one gets  $(y_{O,\infty} - y_{O,0})/(32/12) = y_{P,0}/(44/12) = 1200(T_0 - T_\infty)/(33 \cdot 10^6)$ , with  $T$  in kelvin, what is plotted in Fig. 7b.

### Exercise 1. Partial oxidation of carbon particles at high temperature

## PROPAGATION OF PREMIXED FLAMES

People learnt to make non-premixed flames on torches some 500 000 years ago, but it was only very recently, after R.W. Bunsen conceived his famous burner in 1855, that premixed flames are used, not only in most gas-fired burners (from cooking ranges to industrial furnaces) but also in spark-ignition engines and some gas turbines, because premixed combustion is more energy-intense and less pollutant than non-premixed flames. Premixed flames may be laminar (e.g. lab bunsen burner) or turbulent (industrial burners).

Full mixing of a fuel in air takes a lot of time, even when the fuel is already a gas. For mixing to occur in any reasonable engineering-time-span, it must always be made by turbulent convection. The quickest way is by letting a fine dispersion of liquid fuel (obtained by high-pressure injection) to evaporate and mix with air (as in gasoline engines); gaseous jets are more expensive to produce (require more power for pressurisation) and are less ready to disperse (recall the long bunsen tube).

The degree of mixing in traditional Otto engines (both, for the new port-fuel-injection models and the old carburettor models), is perfect, because there is a lot of time from mixture preparation outside the cylinder to ignition after compression. However, the mixing is not so good in the new direct injection spark ignition engines (DISI, also named GDI for gasoline direct injection), which work with a stratified mixture, since there may be no time enough from injection to ignition; DISI engines (first developed by Mitsubishi in 1995), only admit air to the cylinders (without a throttling valve), and inject fuel within the cylinder during the compression stroke, with the injector (placed near the spark-plug) controlled in such a way that as to have a stratified mixture, only rich near the spark-plug (i.e. easily flammable), which causes the burning of the overall lean mixture (increasing a lot the efficiency on partial loads, one of the weakness of Otto engines).

## LAMINAR COMBUSTION

Perfectly premixed, quiescent flames are the easiest to analyse, the most instructive to study, and a prerequisite to understand any combustion phenomena. Although the most common laminar premixed flame is obtained at the tip of the bunsen burner, it is easier to consider a flame propagating inside a long tube filled with a premixture (e.g. a 10% in volume of methane in air, at ambient temperature and pressure, being ignited by a spark), assuming as a first approximation a planar one-dimensional propagation.

The main feature of premixed flames is their characteristic propagation speed, but there are other attributes that distinguish them from non-premixed flames, none the least their colour: contrary to the yellow colour of non-premixed flames (due to blackbody emission by soot particles), premixed flames show a green-bluish coloration and much lower luminous intensities. This light emission is not due to blackbody radiation because, although the gases are at similar temperature in both types of flames, a huge volume of gas is required to make it optically thick (several metres); otherwise, only some characteristic spectral bands show up over the tenuous bulk emission, those corresponding to the species present. For instance, rich premixed methane/air flames (e.g. as in a cooking range, when some primary air is used) are blue/green due to CH and C<sub>2</sub> radicals, whereas lean premixed methane/air flames are green due to C<sub>2</sub>

radicals. Although the predominant colour in premixed flames is blue, as for methane and natural gas, propane and LPG flames are greener and brighter, and alcohol and hydrogen flames are purple and tenuous.

The additional non-premixed flame surrounding the rich premixed methane/air flame is also blue (and not yellow, as in normal non-premixed flames) because now there is little fuel remaining and consequently soot formation is hindered.

The strong temperature gradient is one of the main characteristic of a flame. Mallard and Le Châtelier proposed in 1883 a model for the propagation of a flame in quiescent premixed gases (laminar deflagration), assuming that the heat-release zone was much smaller than the temperature-change zone (Fig. 8), i.e. just a thermal model, equivalent to the steady-state in the adiabatic motion of a planar heat-source.

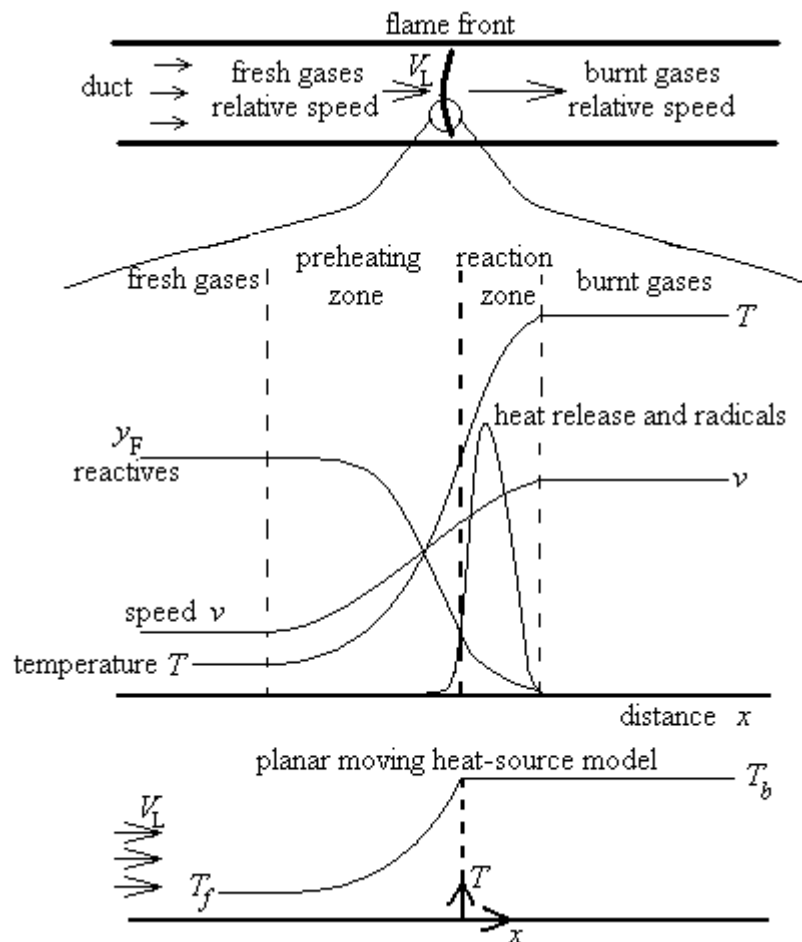


Fig. 8. Internal structure of a premixed laminar flame, and its equivalent thermal model.

In axes moving with the front, the energy balance (heat equation) for a generic unit volume yields:

$$\rho \frac{dh}{dt} = -\nabla \cdot \bar{q}, \quad \rho V_L \frac{dh}{dx} = k \frac{\partial^2 T}{\partial x^2}, \quad V_L \frac{dT}{dx} = a \frac{d^2 T}{dx^2}, \quad \frac{T - T_f}{T_b - T_f} = \exp\left(\frac{x V_L}{a}\right) \quad (34)$$

where for the fresh mixture entering from the left at  $T_f$  and the burnt products exiting to the right at  $T_b$ ; this is valid for  $-\infty < x \leq 0$  (it is  $T = T_b$  for  $x \geq 0$ ). The heat release per unit area is  $\dot{Q}/A = \rho_f V_L c_p (T_b - T_f) \approx 1 \text{ MW/m}^2$  (i.e. some 100 W per square centimetre of flame), having substituted

typical values for density of fresh gases,  $\rho=1 \text{ kg/m}^3$ , for the laminar deflagration speed  $V_L=0.5 \text{ m/s}$ , for the thermal capacity  $c_p=1000 \text{ J/(kg}\cdot\text{K)}$ , and for the temperature increase  $T_b-T_f=2000 \text{ K}$ .

The most important feature of this thermal conduction model is obtained by a mere order of magnitude analysis that shows that the thermal thickness,  $L_{th}$ , is related to the deflagration speed by just  $L_{th}=a/V_L$ , from the exponential argument in (34), i.e., for a mean temperature of 1500 K ( $a=2\cdot 10^{-5} \text{ m}^2/\text{s}$  at room temperature, but at 1500 K  $a=0.35\cdot 10^{-3} \text{ m}^2/\text{s}$ ) one gets  $L_{th}V_L=0.35\cdot 10^{-3} \text{ m}^2/\text{s}$ , what agrees very well with typical values of  $L_{th}=10^{-3} \text{ m}$  and  $V_L=0.4 \text{ m/s}$ . A more refined analysis yields  $L_{th}V_L=2a$ . A further analysis of the laminar deflagration speed  $V_L$  follows.

### Deflagration speed

The laminar deflagration velocity  $V_L$  is the flame-front speed relative to the quiescent, premixed, fresh gases (i.e. the volumetric rate of fresh mixture being burnt, per unit area). Besides,  $V_L$ , it is sometimes named  $S_L$ , for laminar speed, or  $V_b$ , for burning velocity, or  $V_f$ , for flame velocity, or  $V_D$ , for deflagration velocity, etc., but  $V_L$  seems preferable because it reminds of the laminar character (practical combustion is turbulent) and the apparent flame speed may vary with the configuration (e.g. the observable speed of a flame in a tube only coincides with  $V_L$  for the open-exit / closed-intake tube).

The laminar deflagration velocity  $V_L$  varies with type of fuel, type of oxidiser, relative air ratio in the mixture,  $\lambda=A/A_0$ , temperature,  $T_f$ , and pressure,  $p_f$ .

- Effect of fuel.  $V_L$  has a maximum value of near 0.5 m/s for most hydrocarbons:  $V_L=0.45 \text{ m/s}$  for  $\text{CH}_4$ ,  $\text{C}_3\text{H}_8$ ,  $\text{C}_6\text{H}_6$ ,  $\text{CO}$ , but  $V_L=0.75 \text{ m/s}$  for  $\text{C}_2\text{H}_4$ ,  $V_L=0.85 \text{ m/s}$  for  $\text{CH}_3\text{-CH}_2\text{OH}$ ,  $V_L=1.6 \text{ m/s}$  for  $\text{C}_2\text{H}_2$  and  $V_L=3.5 \text{ m/s}$  for  $\text{H}_2$ .
- Effect of oxidiser. It depends on oxidiser composition (air,  $\text{O}_2$ ,  $\text{H}_2\text{O}_2$ ). For air,  $V_L$  increases one order of magnitude from  $x_{\text{O}_2}=0.21$  to  $x_{\text{O}_2}=1$  (e.g.  $V_L=3.9 \text{ m/s}$  for  $\text{CH}_4/\text{O}_2$ ,  $V_L=3.6 \text{ m/s}$  for  $\text{C}_3\text{H}_8/\text{O}_2$ ,  $V_L=3.3 \text{ m/s}$  for  $\text{C}_4\text{H}_{10}/\text{O}_2$ ,  $V_L=7.5 \text{ m/s}$  for  $\text{C}_2\text{H}_2/\text{O}_2$  and  $V_L=14 \text{ m/s}$  for  $\text{H}_2/\text{O}_2$ ). Notice that pure oxygen may give rise to a detonation (see Supersonic combustion, below). Also, for a given  $x_{\text{O}_2}$ ,  $V_L$  varies with the dilutant: with Ar and He it is double than with  $\text{N}_2$ . However, although adding an inert gas lowers the deflagration speed, in some special cases it may act as a positive catalyst and increase it, as in the striking case of  $\text{CO}/\text{O}_2$  combustion, where a 0.2%  $\text{H}_2\text{O}$  causes an eight-fold increase of  $V_L$ . Other striking case is the reduction of  $V_L$  from 2.7 m/s to 0.15 m/s for  $\text{H}_2/\text{air}$  flames when adding 3.5% butane.
- Effect of mixture ratio. Experiments show that  $V_L$  has a maximum value for  $\lambda$  slightly over  $\lambda=1$ , and decreases parabolically towards the ignition limits (to some 30%..10% of its maximum value, not to zero). For premixed methane/air mixtures at ambient conditions,  $V_L$  decreases from  $V_L=0.45 \text{ m/s}$  at  $\lambda=1.05$ , to  $V_L=0.15 \text{ m/s}$  at  $\lambda=0.65$  and at  $\lambda=1.7$ ; a minimum value of  $V_L=0.036 \text{ m/s}$  at  $\lambda=2.08$  has been found under microgravity conditions); Fig. 9 presents additional data.

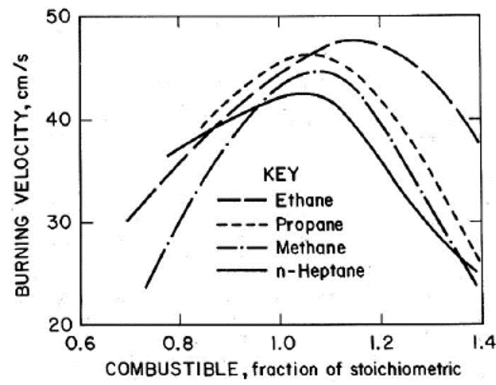


Fig. 9. Laminar deflagration speed vs. equivalence ratio,  $\phi=1/\lambda$ , for some fuels, at room conditions.

- Effect of temperature.  $V_L$  increases exponentially with fresh gases temperature,  $T_f$  (e.g. from  $V_L=0.45$  m/s at 300 K to  $V_L=1.2$  m/s at 600 K).
- Effect of pressure.  $V_L$  decreases with increasing pressure to a half from 100 kPa to 1 MPa (it increases 50% from 100 kPa to 10 kPa). An empirical correlation from Andrews and Bradley for stoichiometric  $\text{CH}_4/\text{air}$  flames is  $V_L = (c_1 + c_2 T^2) / \sqrt{p/p_0}$ , with  $c_1=0.1$  m/s,  $c_2=3.7 \cdot 10^{-6}$  (m/s)/K<sup>2</sup> and  $p_0=100$  kPa.

Some prediction of all the above-described  $V_L$ -dependence may be obtained following the thermal model above. The burning rate density,  $\dot{\xi}/V$ , must be proportional to the overall concentration of fresh gases,  $c_f=p/R_u T_f=\rho_f M_m$ , and inversely-proportional to the time taken to burn the gases inside the flame thickness, i.e. to  $t_{th}=L_{th}/V_L$ , so that, upon substitution of  $L_{th}V_b=a$  in  $\dot{\xi}/V=c_f/t_{th}$  and elimination yields:

$$V_L = \sqrt{\frac{a}{c_f} \frac{\dot{\xi}}{V}} = \sqrt{a \frac{M_m}{\rho_f} \left( \frac{-dc_F}{dt} \right)} \quad (35)$$

or with a more refined analysis:

$$V_L = \sqrt{a(1+\nu_O) \frac{M_F}{\rho_f} \left( \frac{-dc_F}{dt} \right)} \quad (36)$$

where  $M_m$  and  $M_F$  are the molar masses of the mixture and the fuel,  $\nu_O$  is the stoichiometric mass coefficient for the oxidiser ( $\text{O}_2$ ) relative to unit mass of fuel (e.g.  $\nu_O=15.6$  for methane in air),  $\rho_f$  the unburnt mixture density, and  $dc_F/dt$  the speed of reaction for the fuel. But the effect of the chemical kinetics is difficult to guess beyond Arrhenius's law and the law of mass action.

There are many procedures to measure laminar deflagration speeds, usually grouped in stationary and moving flames. For planar geometries, a flame stabilised over a porous burner is better than the travelling flame along a tube, since the effect of gravity on the later, gives way to different speeds for upward and downward propagation, and a non-symmetric parabolic flame in horizontal propagation, increasing the burning area and the speed. For cylindrical geometries, the typical bunsen flame may be used, and better if a planar velocity profile for the issuing jet is achieved by a contraction (in any case, the overall injection speed, times the cross-section area, divided by the flame area, gives a  $\pm 20\%$  approximation to

the deflagration speed). For spherical geometries, central ignition inside a soap bubble filled with a premixed fuel/air mixture may be used.

The laminar deflagration speeds here consider refer to open flames. Flames inside porous media have higher values; e.g. for methane/air, maximum deflagration speed increases from 0.45 m/s in free-flames to 4 m/s in porous-media flames, explained because of the 10-fold increases in thermal diffusivity  $a$  (100 times in  $k$ , but 10 times in  $\rho c$ ).

It is important to keep in mind that the products leave the flame at a quicker pace than the deflagration speed, due to the effect of temperature on mass conservation. For instance, in the planar geometry,  $\rho_f V_L = \rho_b v_b$ , i.e.  $v_b/V_L = (p_f/p_b)(M_f/M_b)(T_b/T_f)$ , where the last factor in the right-hand-side product is the dominant (of order 7 or 8, the other two being of order 1). Thus, for a typical 0.4 m/s flame speed towards the fresh gases, the products are ejected at some 2.5 m/s to the other side.

It must be reminded that all this refers to the laminar speed; propagation speed greatly increases (parabolically) with Reynolds number in the turbulent regime, what is profitably used in practical systems (typical turbulent speeds are some 5 times larger than the laminar speed).

### Flame thickness

The flame front is very thin, in either premixed or non-premixed flames; usually less than a millimetre. Some comments made when analysing non-premixed flame lengths, apply also here: the uncertainty in measuring the thickness of a solid sheet is well understood, even for an elastic material, but, what about for the thickness of a gaseous layer as in a flame? One possible answer may be its thermal thickness (once we agree on a certain norm, e.g. the mean distance between points with temperature say 1% greater than the entering fresh mixture and the points with temperature say 1% lower than the exiting products, from a temperature profile as in Fig. 8). But another possibility may be its light-intensity thickness (once we agree also on a certain norm, e.g. using a certain photographic plate, or a given monochromatic band, and the threshold levels); or some chemical thickness; etc. The visible thickness is always smaller than the thermal thickness (say one half), and the visible layer stays at the downstream-end of the thermal layer (see Fig. 8), there where radicals recombine.

As reasoned before, the thermal thickness,  $L_{th}$ , is related to the deflagration speed by just  $L_{th}V_L = a$ , with typical values of 1 mm, that may grow to 1 cm at very low pressures (10 kPa). This applies to near-stoichiometric deflagration speeds; outside that range, flame thickness grows parabolically (e.g. for premixed methane/air mixtures at ambient conditions,  $L_{th}$  grows from 1 mm at  $\lambda=1$ , to  $L_{th}=10$  mm at  $\lambda=0.6$  and at  $\lambda=2$ ).

To help develop appropriate kinetic models, it is very important to diagnose the species production rate profiles within the flame. The main reactives (fuel and oxygen) show a simple consumption rate profile (say a Gauss bell in the  $dc_i/dt$  profile), similar to the main products ( $H_2O$  and  $CO_2$ ), that show a simple production rate profile, whereas  $CO$ ,  $NO_x$  and radicals show first a neat production rate profile, followed

by a less pronounced consumption rate profile, that, if there is not enough time to equilibrium, causes a neat production and consequent emission.

### Flame stabilisation

Contrary to non-premixed flames, that naturally stabilise at the shear layer between fuel and oxidiser because they cannot propagate to one side or the other, premixed flames have their own propagation speed and, when fed with the fresh mixture, except in a very short range of matching the propagation speed, they tend to flashback or blowoff. For instance, if a stable CH<sub>4</sub>/air premixed-flame is to be realised at the mouth of a bunsen burner, the mixture (within its ignition limits) must be fed between twice and five times the laminar deflagration speed.

Several methods are employed to stabilise a partially or totally premixed flame a desired location in a combustor, against natural uncontrolled fluctuations and the intended operation range, all methods trying to procure a region where natural flame speeds are matched:

- Sudden flow expansion, giving rise to detached flows with a vast range of speeds.
- Swirling by jet induction or bypass flows, giving rise to a recirculation with a vast range of speeds
- Bluff-bodies, given way to a vast range of speeds at their wakes.
- Local hot spots (e.g. ceramics with large thermal inertia) that permanently ignite the mixture.

The trade-off between flame stability (greater for non-premixed flames) and flame energy intensity (greater for premixed flames) is usually solved by a sequential combination of a premixed flame and a non-premixed flame; i.e. some primary air is added to the fuel (more than the lower flammability limit and less than the stoichiometric ratio), a premixed flame is established, and the remaining fuel is burnt in a second non-premixed flame with another supply of air (e.g. from the ambient). These partially-premixed combined flames are the usual feature in bunsen burners and domestic gas-stoves and gas-heaters. Their stability diagram, in terms of the primary air (that used in the premixed flame) is presented in Fig. 10.

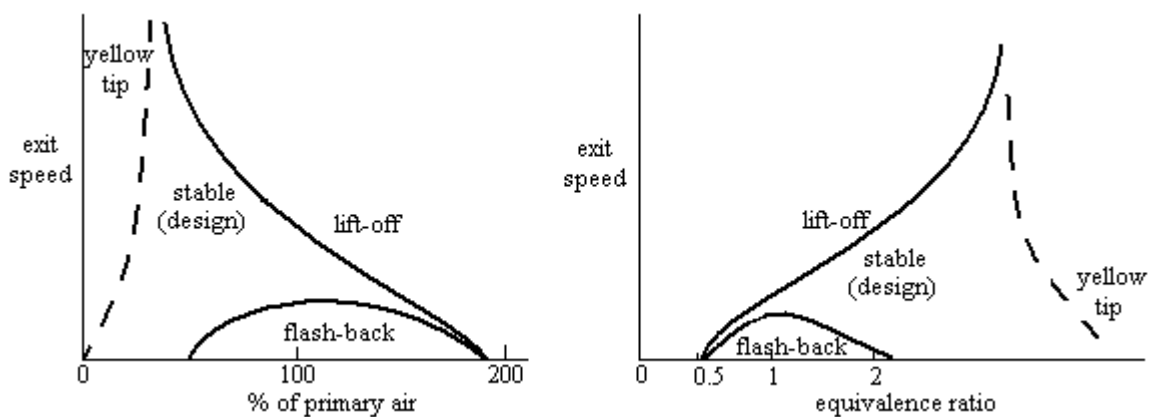


Fig. 10. Stability of bunsen flames in terms of primary air. When both, fuel and air are supplied the stability diagram is presented in terms of the equivalence ratio of the mixture supplied.

The easiest way to light a bunsen is with the primary-air openings closed (0% primary air, infinite equivalence ratio of the feeding mixture) because this flame is most stable (it would detach only at an order of magnitude larger exit speeds); but this flame is very long and yellow, and a better combustion can be achieved by increasing the primary air to 60% or 70% of the stoichiometric (i.e. increasing the

relative air/fuel ratio  $\lambda$  to 0.6 or 0.7, or decreasing the equivalence ratio  $\phi$  to 1.8 or 1.5). Lean mixtures are more unstable, and, if more air than that corresponding to the lower flammability limit is supplied, the mixture cannot be ignited at room temperature.

### Flame quenching

Quenching is the extinction of a flame by an excessive heat-loss towards relatively-cold solid boundaries nearby. Quenching prevents the propagation of combustion along narrow tubes or orifices and through fine wire-meshes (see Fig. 11). Quenching distance is typically of 2 mm for normal hydrocarbon flames (e.g. for stoichiometric fuel/air mixtures at 100 kPa and 20 °C,  $d_Q=1.9$  mm for CH<sub>4</sub>,  $d_Q=2.1$  mm for C<sub>3</sub>H<sub>8</sub>,  $d_Q=2.0$  mm for n-C<sub>8</sub>H<sub>18</sub>,  $d_Q=1.8$  mm for CH<sub>4</sub>O but  $d_Q=0.6$  mm for H<sub>2</sub>). These values increase with the air/fuel ratio outside the minimum value (corresponding to  $\lambda \approx 0.9$ ), and decrease with pressure, with corrugation (non-circular ducts have slightly lower values), with temperature (the quenching effect is lost at high temperature, as in combustion within porous media), and with the presence of catalysts. Domestic gas-fired appliances usually have multi-hole or multi-blade burners (slightly corrugated slots to increase mechanical stiffness), with passage sizes below 3 mm to prevent flame ingestion.

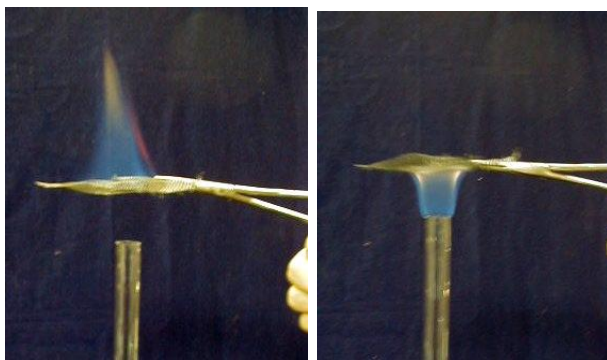


Fig. 11. A fine wire mesh prevents flame propagation through, so that if the premixed jet is ignited at one side of the mesh, the flame cannot traverse to the other side.

### Flammability limits

Non-premixed flames are very stable in the sense that, once ignited, they tend to stay anchored to the burner under most variable circumstances, but a premixed fuel/air mixture may not propagate a local combustion (e.g. by a spark stimulation) if there is too-much air or too-much fuel, because a certain energy balance must be accomplished between the chemical energy release and heat transfer.

The amounts of gaseous fuel (usually in volume terms in the mixture) between which a flame propagates in a quiescent mixture at ambient conditions, excited by a spark of some 10 J, are called flammability limits (also ignition or explosive limits), defining a flammability range. The lower (or lean) flammability limit, LFL (also known as lower explosive limit LEL, or lower ignition limit LIL), is of greater interest than the upper flammability limit, UFL (or rich flammability limit or upper explosion limit, or upper ignition limit), since, if the fuel molar fraction is lower than  $x_{LFL}$  there is no further risk of accidental combustion, but if it is greater than  $x_{UFL}$ , a subsequent escape of mixture will yield flammable mixtures with omnipresent air.

Some typical flammability limits are presented in Table 2. Common units for LFL and UFL are molar units, i.e. fuel molar fraction in the gaseous mixture, or, what is the same, in percent volume, %vol. Those

values can be converted to other units: e.g. for methane,  $\{x_{LFL}=5\%, x_{stq}=9.5\%, x_{UFL}=14\%\}$  from [Mass diffusivity data](#), may be expressed also in terms of equivalent ratios  $\{\phi_{LFL}=0.5, \phi_{stq}=1, \phi_{UFL}=2\}$ , relative air/fuel ratios  $\{\lambda_{UFL}=0.5, \lambda_{stq}=1, \lambda_{LFL}=2\}$ , molar air/fuel ratios  $\{A_{UFL}=5.7, A_{stq}=9.52, A_{LFL}=19\}$ , mass air/fuel ratios  $\{A_{UFL}=10, A_{stq}=17.2, A_{LFL}=34\}$ , etc. Le Châtelier proposed in 1898 a rule to compute the lower flammability limit for a mixture of gaseous fuels of molar fractions  $x_i$ :  $x_{LFLm}=1/\Sigma(x_i/x_{LFLi})$ , where only the  $x_i$  of the actual fuels, not of the possible inert components, must be considered.

Table. 2. Flammability limits (in %vol) for premixed fuel/air gaseous mixtures at 25 °C, minimum quenching diameter at 25 °C, and autoignition temperature, all at 100 kPa. Additional data in [Wiki](#).

Fuel	Lower Flammability Limit, LFL	Stoichiometric mixture	Upper Flammability Limit, UFL	Minimum quenching distance [mm]	Autoignition temperature [K]
CO, carbon monoxide	14	29.5	70		900
H <sub>2</sub> , hydrogen	3.9	29.5	75	0.61	850
CH <sub>4</sub> , methane	4.9	9.47	14	2.0	850
C <sub>2</sub> H <sub>6</sub> , ethane	3.0	5.64	13	1.8	800
C <sub>3</sub> H <sub>8</sub> , propane	2.0	4.02	9.5	1.8	750
C <sub>4</sub> H <sub>10</sub> , n-butane	1.5	3.13	8.5		700
C <sub>7</sub> H <sub>16</sub> , n-heptane	1.1	1.87	6.7		560
C <sub>8</sub> H <sub>18</sub> , n-octane	1.0	1.65	6		500
C <sub>8</sub> H <sub>18</sub> , iso-octane	0.95	1.65	6		690
C <sub>10</sub> H <sub>22</sub> , n-decane	0.80	1.34	5.4	2.1	480
C <sub>12</sub> H <sub>26</sub> , n-dodecane	0.60	1.12			480
C <sub>2</sub> H <sub>2</sub> , acetylene	2.5	7.75	80	2.3	600
CH <sub>4</sub> O, methanol	6.7	12.3	36	1.5	680
C <sub>2</sub> H <sub>6</sub> O, ethanol	3.3	6.54	19		630
C <sub>4</sub> H <sub>10</sub> O, ether	1.8	3.13	37		440

Notice that for a liquid fuel tank at room conditions, three cases can be considered for the flammability risk (e.g. in the event of an electrostatic spark inside the tank), according to its equilibrium vapour pressure,  $p_F^*(T)$ : fuels with vapour pressure lower than  $x_{LFL}p$  pose no spark-risk (e.g. diesel oil, fuel oil), fuels with vapour pressure  $x_{LFL}p < p_F^*(T) < x_{UFL}p$  pose a great spark-risk (e.g. methanol, ethanol), and fuels with vapour pressure  $p_F^*(T) > x_{UFL}p$  pose no spark-risk inside the tank (e.g. gasoline, ether, acetone), although in the latter case the venting gases will be flammable when in contact with more air. Another way to verify this tank-flammability behaviour is to put some liquid fuel in an Erlenmeyer flask (e.g. 5 cm<sup>3</sup> in a 100 cm<sup>3</sup> beaker), close it, agitate, open it, and approach a lighter flame; diesel oil will not burn, gasoline burns with a non-premixed flame outside the beaker, and methanol burns violently inside the flask (without explosion because of the wide-enough opening).

Flammability limits above refer to fuel and air at room temperature and pressure conditions. The effects of changes in these parameters are:

- With pure oxygen, the upper flammability limit increases a lot, not so the LFL (e.g. for H<sub>2</sub>/O<sub>2</sub> the change is from  $x_{FL}=4..75\%$ vol to  $x_{FL}=4..95\%$ vol, for CH<sub>4</sub>/O<sub>2</sub> the change is from  $x_{FL}=5..14\%$ vol to  $x_{FL}=5..60\%$ vol, for C<sub>2</sub>H<sub>6</sub>/O<sub>2</sub> the change is to  $x_{FL}=3..66\%$ vol, for C<sub>3</sub>H<sub>8</sub>/O<sub>2</sub> to  $x_{FL}=2..45\%$ vol, for C<sub>4</sub>H<sub>10</sub>/O<sub>2</sub> to  $x_{FL}=1.5..40\%$ vol and for C<sub>2</sub>H<sub>2</sub>/O<sub>2</sub>  $x_{FL}=2.5..95\%$ vol).
- With the addition of an inert gas, the flammable range gets smaller, up to a point where the mixture is no longer flammable at room conditions; e.g. for CH<sub>4</sub>/air mixtures, this point is reached

with 21% of CO<sub>2</sub> in volume, or 26% of water vapour, or 35% N<sub>2</sub>, or 48% He. Notice that for CH<sub>4</sub>/O<sub>2</sub> mixtures up to 80% N<sub>2</sub> may be needed to have a non-ignitable mixture (Fig. 12).

- With temperature, the flammable range gets slightly wider (particularly along the rich side) up to an autoignition temperature (depending on pressure and composition) where any mixture ratio will burn. For instance, for H<sub>2</sub> at 300 °C  $x_{FL}=2.4..83\%$ vol, or for CH<sub>4</sub> at 300 °C  $x_{FL}=3.8..17\%$ vol.
- With pressure, the flammable range widens: e.g., for methane/air,  $x_{LFL}=4.9\%$  and  $x_{UFL}=14\%$  at 0.1 MPa,  $x_{LFL}=3.8\%$  and  $x_{UFL}=55\%$  at 10 MPa, and  $x_{LFL}=3.1\%$  and  $x_{UFL}=60\%$  at 20 MPa.

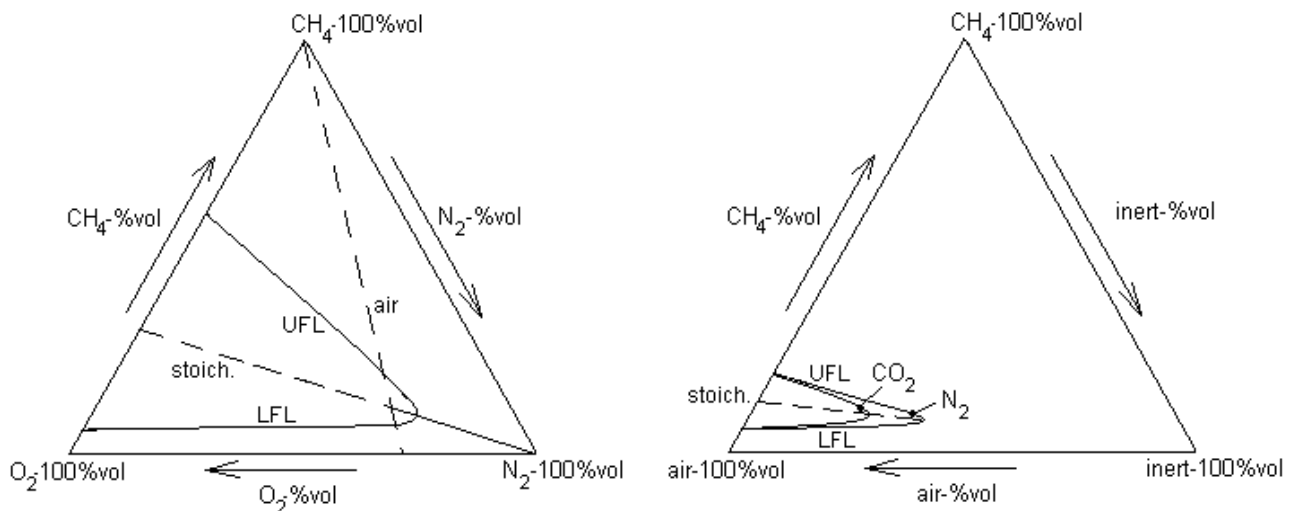


Fig. 12. Influence of an inert gas on the flammability limits of CH<sub>4</sub>/air and CH<sub>4</sub>/O<sub>2</sub> mixtures at room conditions, known as [flammability diagrams](#) (they can be used to find the [minimum oxygen concentration](#) below which combustion is not possible).

### Autoignition temperature

A premixed fuel/oxidiser mixture will spontaneously burn at elevated temperature irrespective of pressure, composition, size, etc. The minimum temperature for this to occur at 100 kPa in air is called autoignition temperature (also known as spontaneous ignition temperature, SIT, some values of which can be found in Table 2). Autoignition is related to heat release and dissipation; according to van't Hoff,  $T_{\text{autoign}}$  is just the temperature at which the rate of generation of heat becomes greater than its rate of dissipation. Substitution of oxygen for air has little effect on autoignition temperature (e.g. 850 K for methane/air and 825 K for methane/oxygen), implying the process is governed more by the Arrhenius expression than by concentrations.

Combustion in this case is not by a flame spatially propagating but by homogeneous combustion of the whole volume at once. A non-premixed fuel/oxidiser mixture will also start burning at high temperature, but here the propagation is as for normal non-premixed flames: at the rate of supply. Practical use of that is made in diesel engines, where intake air is quickly compressed to get it hot enough for the fuel to burn by contact with the hot air, and in some steady combustors where high exhaust-gas-recirculation rates yields high-enough intake temperatures. In reality, some premixed combustion takes place in diesel engines too, since some fuel gets vaporised and mixed with air before autoignition actually occurs (that is why a two-function [Weibe model](#) best fit actual pressure plots). Moreover, in the new dual-fuel diesel engines, a lean premixture (prepared with a high-octane fuel at intake pressures) is fed to the cylinders (with relative air/fuel ratio in the range  $\lambda=0.15..0.45$ , outside the flammability range), compressed below

its high autoignition temperature (e.g.  $<850$  K for natural gas) and made to burn by compression ignition of a minute injection at high pressure of low-autoignition-temperature fuel (e.g.  $>480$  K for diesel oil).

Autoignition may be a hazard in some special cases at low temperature: phosphorus has an autoignition temperature of only  $T_{\text{autoign}}=34$  °C, carbon disulphide has  $T_{\text{autoign}}=90$  °C, diethyl ether has  $T_{\text{autoign}}=160$  °C (it can be ignited by a hot plate), sulfur has  $T_{\text{autoign}}=240$  °C, etc. Additionally, it must be recalled that the quoted autoignition temperatures refer to sudden inflammation, but, if the system is well insulated, autoignition may occur at much lower temperatures after some self-heating period (e.g. a  $\text{H}_2/\text{air}$  mixture will suddenly burn by itself at some 850 K, but it has been reported that in well insulated envelopes it self-ignites after a couple of hours at 750 K).

## SUPERSONIC COMBUSTION

Combustion is a slow process (think of the maximum premixed laminar flame speed of 0.45 m/s for methane/air, or the slow burning of wood in the fireplace). High burning rates required in engineering applications, due to short residence time dictated by kinematics in reciprocating engines or size in other combustors, are achieved by promoting turbulence (e.g. in a gas turbine combustor the average speed is some 50 m/s, two orders of magnitude larger than typical laminar flame speeds, without the flame being blow-off (aided by some flame-holder devices). But, could the flame speed be raised to say 2000 m/s? The answer is yes, supersonic combustion sometimes takes place accidentally in coal mines and other closed places, as well as within condensed explosives, but no controlled application has been developed yet.  $\text{H}_2/\text{O}_2$  and  $\text{C}_2\text{H}_2/\text{O}_2$  mixtures are particularly prone to detonation. Notice that the ignition limits for supersonic combustion are usually narrower than for deflagration; e.g. for  $\text{H}_2/\text{air}$  premixed combustion, the flammability limits change from  $x_{\text{FL}}=4..75\%$ vol to detonability limits of  $x_{\text{DL}}=18..59\%$ vol.

Supersonic combustion, called detonation, is realised coupled to a shock wave travelling at supersonic speed. Deflagration to detonation transition (DDT) is difficult to understand. If premixed gases inside a tube closed at both ends are ignited at one end, a laminar flame first develops, travelling fast being pushed by the expanding hot products behind. The inverted small pressure-jump across the flame generates local pressure pulses that wrinkles the flame, creates turbulence, extends the burning area and increases the burning rate, with a positive feedback that, if positively combined with pressure pulses reflected from the other end, might compress the fresh mixture to the autoignition temperature.

Although it is very difficult to have a planar geometry in practice (both in subsonic and supersonic combustion), we analyse just the planar case because it yields the maximum benefit/cost for learning.

For a planar fluid front, be it a subsonic deflagration, a sonic acoustic wave, a supersonic shock wave, or a supersonic combustion behind a shock wave, the mass, momentum and energy balance equations through it at a steady state are:

$$\rho_1 v_1 = \rho_2 v_2 = \dot{m}_A \quad (37)$$

$$p_1 + \rho_1 v_1^2 = p_2 + \rho_2 v_2^2 \quad (38)$$

$$h_1 + \frac{v_1^2}{2} + q = h_2 + \frac{v_2^2}{2} \quad (39)$$

where  $\dot{m}_A$  is the mass-flow-rate per unit area traversing the front, and  $q=y_F \text{PCI}$  is the heat release equivalent to the chemical energy of combustion (if there is such), that is taken apart from the thermo-mechanical enthalpy  $h$ .

The intention is to analyse the possible exiting conditions for a given entry conditions, what is traditionally visualised in the pressure-volume diagram ( $p$ - $v$ , or better  $p$ - $1/\rho$ , in terms of density, since we keep  $v$  for velocities).

From (37) and (38) one gets the so called Rankine line (a straight line in the  $p$ - $1/\rho$  diagram):

$$p_2 - p_1 = -(\rho_2 v_2^2 - \rho_1 v_1^2) = -\left(\frac{1}{\rho_2} - \frac{1}{\rho_1}\right) \dot{m}_A^2 \rightarrow \frac{dp_2}{d\frac{1}{\rho_2}} = -\dot{m}_A^2 \quad (40)$$

showing that, for a given entry conditions (point A in Fig. 13) the only possible exiting conditions lay in the second and fourth quadrant from A, since  $\dot{m}_A$  is always positive.

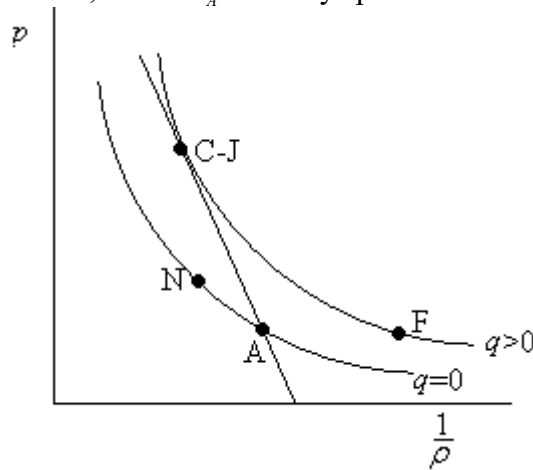


Fig. 13. Possible exiting conditions (Rankine straight line) after a planar fluid wave, in the pressure-volume diagram, for a given entry conditions at point A. After a normal flame, point F is reached (the Rankine line would join A and F). Acoustic waves take place as oscillations around point A along  $q=0$  (the Rankine line would be the local tangent). Normal chock waves correspond to points like N (the Rankine line would join A and N). A detonation corresponds to point C-J (Chapman-Jouguet), the tangent point for the Rankine line from A to the Hugoniot curve  $q>0$  (positive heat release).

From (37), (38) and (39) one gets the so called Hugoniot curve (or Rankine-Hugoniot curve):

$$h_2 - h_1 = q - \left(\frac{v_2^2}{2} - \frac{v_1^2}{2}\right) = q - \frac{v_2 + v_1}{2} (v_2 - v_1) = q + \frac{v_2 + v_1}{2} \frac{p_2 - p_1}{\rho_1 v_1} = q + \frac{p_2 - p_1}{2} \left(\frac{1}{\rho_2} + \frac{1}{\rho_1}\right) \quad (41)$$

that, with the perfect gas model ( $\Delta h = c_p \Delta T$ ,  $T = p/(\rho R)$ ,  $c_p/R = \gamma/(\gamma-1)$ ) yields:

$$\frac{\gamma}{\gamma-1} \left(\frac{p_2}{\rho_2} - \frac{p_1}{\rho_1}\right) = q + \frac{p_2 - p_1}{2} \left(\frac{1}{\rho_2} + \frac{1}{\rho_1}\right) \quad (42)$$

that, although not evident, corresponds to a kind of hyperbolic curve in the  $p-1/\rho$  diagram (Fig. 13), displaced to the right of point A because of the  $q$  term (always positive).

In the case of a normal flame, the jump through the front is from A to F, with a small pressure drop (some 2%) and a large specific-volume increase (some 7 times).

The case of acoustic waves correspond to small departures to the left of A along the curve for  $q=0$ . Assuming negligible energy dissipation, the process is isentropic, and from the differential forms of equations (37) and (38),  $d(\rho v)=0$  and  $dp+d(\rho v^2)=0$ , one gets the general equation for the speed of sound:

$$dp + d\left(\frac{\rho^2 v^2}{\rho}\right) = dp + \rho^2 v^2 d\left(\frac{1}{\rho}\right) = 0 \rightarrow \frac{dp}{d\rho} = v^2 \rightarrow v_{\text{sound}} = \sqrt{\left.\frac{\partial p}{\partial \rho}\right|_S} \stackrel{\text{PGM}}{=} \sqrt{\gamma RT} \quad (43)$$

where the particularisation for the perfect gas model (PGM) can simply be obtained from differentiating the logarithm of  $(p/\rho)^\gamma = \text{constant}$ .

The case of a normal shock wave correspond to large departures to the left of A along the curve for  $q=0$ . Substituting  $\rho = p/(RT)$  and  $v = M\sqrt{\gamma RT}$  in equations (37), (38) and (39) for the perfect gas model,  $M$  being the Mach number  $M \equiv v/v_{\text{sound}}$ , one gets:

$$\rho v = \frac{p}{RT} M \sqrt{\gamma RT} \rightarrow \frac{pM}{\sqrt{T}} = \text{constant} \quad (44)$$

$$p + \rho v^2 = p + \frac{p}{RT} M^2 \gamma RT = p(1 + \gamma M^2) = \text{constant} \quad (45)$$

$$h + \frac{v^2}{2} = c_p T + \frac{M^2 \gamma RT}{2} \rightarrow T \left(1 + \frac{\gamma - 1}{2} M^2\right) = \text{constant} \quad (46)$$

from which one may get an explicit expressions for the exiting Mach number:

$$M_2 = \sqrt{\frac{2 + (\gamma - 1)M_1^2}{2\gamma M_1^2 - (\gamma - 1)}} \quad (47)$$

and, upon substitution, the rest of the variables. Notice, by the way, that the Hugoniot curve must lay to the right of the isentropic curve  $(p/\rho)^\gamma = \text{constant}$  passing by A, since there can only be entropy increases in real adiabatic processes.

Finally, for the detonation case, the exiting conditions correspond precisely to the Chapman-Jouguet point (C-J in Fig. 13); the rationale is that, if it were above C-J, the exiting velocity would be subsonic and the combustion would not be able to sustain that strong shock wave, whereas if it were below C-J, the exiting velocity would be supersonic and the combustion would tend to accelerate the shock wave; that is why it is found in practice that detonation waves always approach the C-J point. The internal structure of the detonation can be separated in a very thin leading region (a few molecular free-paths) of a strong shock

with a pressure jump of say 40-fold (and temperature and density jumps of say 7-fold and 5-fold, respectively) leaving the stream subsonic with a local  $M \approx 0.4$ , followed by a much thicker combustion region where the fluid accelerates towards the local sonic speed  $M=1$  while increasing further the temperature and decreasing both pressure and density. For a stoichiometric methane/air mixture at ambient conditions, the detonation velocity is 1800 m/s (advancing speed relative to quiescent fresh gases), varying little with pressure and composition and more with temperature, the corresponding Mach number is  $M_1=5.1$ , and the exiting temperature and pressure 2780 K and 1.72 MPa..

## TURBULENT COMBUSTION

Combustion usually takes place in a turbulent flow, from combustion chambers in gas turbines, boilers and furnaces, to reciprocating engines and uncontrolled fires. But, as in Fluid Mechanics, a larger share of the learning effort is devoted to study laminar flows because they are more amenable, and more advanced turbulent models are presently built upon them.

The basic characteristic of turbulence is that all local variables (velocities, pressure, temperature, concentrations) show a random fluctuation superimposed to a running average changing more slowly (or being constant if the flow is steady in the average; turbulence is always unsteady in the detail). This randomness does not mean the flow is not deterministic; it means that the flow is too sensitive to uncontrolled initial and boundary perturbations. In pipe flow, for instance, turbulent slugs may appear at low Reynolds number ( $Re \sim 200$ ), decaying more slowly the higher this value, until at  $Re \sim 2300$  they no longer decay in most setups; but in very smooth walls, smooth entry and quiet environment, the laminar regime has been maintained up to  $Re \sim 100\ 000$ .

Turbulence introduces a very effective exchange of mass, momentum and energy in cross-stream directions, increasing physical transport by orders of magnitude, what is a blessing in engineering problems limited by the mixing rate, as in combustion (obviously for non-premixed flames, but also for extending the flame front in premixed flames, and for the dispersion of pollutant emissions).

For instance, for a velocity component  $u$ , along a given direction,  $x$ , a very quick scanning (e.g. laser-doppler, hot-wire or ultrasonic velocimetry) would yield a fluctuating variable  $u(t,x,y,z)$  at a given point  $(x,y,z)$ . But  $u(t)$  is aperiodic and its average would depend on the time-span considered,  $\Delta t$ . In practice, one can find suitable  $\Delta t$  values that depend on the problem at hand; for typical engineering problems it may be  $\Delta t < 10^{-2}$  s, i.e. fluctuations below  $10^2$  Hz are retained, and above that are averaged), whereas for meteorological problems it may be  $\Delta t \approx 10^3$  s, i.e. fluctuations below  $10^{-3}$  Hz are retained, and above that are averaged). The theoretical value for  $\Delta t$  would be determined by the autocorrelation of the function being averaged. Assuming  $\Delta t$  is well defined, the fluctuating variable could be decomposed in a running mean,  $\bar{u}$ , and a random fluctuation  $u'$ :

$$u = \bar{u} + u' \quad \text{with} \quad \bar{u} = \frac{1}{\Delta t} \int_t^{t+\Delta t} u dt \quad (48)$$

inst.
mean
fluct.

Turbulence theories try to model this statistic problem by reducing the number of representative parameters. Unfortunately, the non-linear convective term in Navier-Stokes equations make the statistic analysis non-linear, introducing higher-order coupling terms at any stage in the decomposition problem, giving rise to a closure problem. For instance, the momentum equation along  $x$  for incompressible flow, when averaged, reduces to:

$$\begin{aligned} \frac{\partial(\rho(\bar{u}+u'))}{\partial t} + \nabla \cdot (\rho(\bar{u}+u')(\bar{v}+\bar{v}')) &= -\frac{\partial(\bar{p}+p')}{\partial x} + \rho g_x + \mu \nabla^2(\bar{u}+u') \\ \rightarrow \frac{\partial(\rho\bar{u})}{\partial t} + \nabla \cdot (\rho\bar{u}\bar{v}) + \nabla \cdot (\rho\overline{u'v'}) &= -\frac{\partial(\bar{p})}{\partial x} + \rho g_x + \mu \nabla^2\bar{u} \end{aligned} \quad (49)$$

since the mean of single random variables is zero. The new term appearing in turbulent flows (the third in the left hand side) may be transposed to the right-hand-side of (49) and thence it is called turbulent Reynolds stress, defining an empirical turbulent viscosity,  $\mu_t$ , usually much larger than the viscous one):

$$-\nabla \cdot (\rho\overline{u'v'}) \equiv \mu_t \nabla^2 \bar{u} \quad (50)$$

Turbulence is always a three-dimensional spatial-temporal problem, and thus spatial and temporal correlations are sought. The parameters introduced to quantify turbulence are of two types:

- Turbulent intensities of the variables, i.e. root-square-means in the temporal fluctuations of velocities, temperature, concentrations...), that may be of the same order as the mean values.
- Turbulent scales in the coordinates, defining a region of fluid with correlated properties (an eddy or vortex, since turbulent motion is highly rotational), that may be of the same order as the geometrical size of the problem.

Several length scales may be defined in turbulent flows; from the largest to the smallest: the main length of the geometry,  $L$  (e.g. the diameter in a pipe flow), the large-eddy scale,  $L_{LE} = \int_{r_0}^{\infty} \overline{u'(r_0)u'(r)} dr / (u'_{rms}(r_0)u'_{rms}(r))$ , the Taylor mesoscale,  $L_{TY} = u'_{rms} / (\partial u' / \partial y)_{rms}$ , and the Kolmogorof microscale,  $L_{KG} = (\nu^3 / \varepsilon)^{1/4} = [\nu^3 (L_{LE} / u'_{rms}) / ((3/2)u'^2_{rms})]^{1/4}$  (where  $\nu$  is the kinematic viscosity and  $\varepsilon$  the energy dissipation rate,  $\varepsilon = \nu (\sum \partial u_i' / \partial x_i)_{rms}$ ), beyond which there is no further convective-transport but viscous-dissipation. Associated Reynolds numbers are defined as  $Re_L = uL/\nu$ ,  $Re_{LE} = u'_{LE}/\nu$ ,  $Re_{TY} = u'_{TY}/\nu$  and  $Re_{KG} = u'_{KG}/\nu$ , with the ratios  $L_{LE}/L_{TY} = Re_{LE}^{3/4}$  and  $L_{LE}/L_{KG} = Re_{LE}^{1/2}$ . In reality, there is a continuum in length scales (the turbulent cascade) and in time scales (the frequency spectrum of energy distribution is continuum), all due to the non-linear character of turbulence.

Several turbulent intensities may be defined in turbulent flows: the eddy viscosity just introduced in (50),  $\mu_t$ , the relative turbulent intensity,  $i_u \equiv u'_{rms}/\bar{u}$ , the specific turbulent kinetic energy,  $k \equiv u'^2_{rms}/2$ , the turbulent mixing length,  $\ell_m$  (defined by  $\mu_t = \rho \ell_m^2 \partial(\bar{u})/\partial y$ ), the turbulent kinetic energy dissipation rate,  $\varepsilon$ , etc.); the traditional  $k-\varepsilon$  model is widely used. More elaborated models are being tried, as the Reynolds stresses model in terms of ternary correlations, the large-eddy simulation (where only smaller scales are averaged) and the direct numerical simulation of the whole statistical problem (only affordable for academic configurations).

Trying to render the formulation of real turbulent flows more amenable, some of the following simplifications may be imposed on the model:

- Steady turbulence, when  $du'_{rm}/dt=0$  for all fluctuating components.
- Homogeneous turbulence, when  $du'_{rm}/dx=0$  for all fluctuating components in all directions.
- Isotropic turbulence, when  $du'_{rm}/d\theta=0$  for all fluctuating components in all angular directions. Sometimes only local lateral isotropy is imposed, i.e. two turbulent intensities are retained: the axial one along the local mean velocity, and the lateral one (assumed isotropic).

### Axisymmetric turbulent jet flames

Perhaps the more representative case of turbulent flow in combustion is the turbulent jet. When one stream issues into an otherwise quiescent fluid (gas in gas, or liquid in liquid; the case of a liquid in a gas being very different), the incoming stream detaches at the exit lip, becoming a predominantly axial flow (jet) that decays along the axial length while entraining external fluid and broadening in a more-or-less conical flow; i.e. for large distances compared to the exit diameter,  $D_0$ , there is a conical similarity solution in  $r/z$ . The radius where the axial speed is half of the central speed,  $r_{1/2}$ , or either where it is 1%,  $r_{99}$ , is used to characterise the width of the jet.

- For laminar flows ( $Re=w_0D_0/\nu < 1000$  or even  $Re < 10$  for non-parabolic jets) the semi-angle is small and given by  $r_{1/2}/z = 6/Re$  (e.g.  $3.5^\circ$  for  $Re=100$ ), with the central speed decreasing hyperbolically as  $w = (3/32)(w_0D_0/z)Re$ . This conical solution is only valid for  $z/D_0 > 9$ .
- For turbulent flows,  $Re > 2000$ , the semi-angle is larger (typically  $9^\circ$ ), with the central speed decreasing hyperbolically as  $w = 6.6w_0D_0/z$ , both independent of the Reynolds number. This conical solution is only valid from  $z/D_0 > 8$  to  $z/D_0 < 100$  with the origin at  $z/D_0 = 0.6$ .

Non-premixed combustion of an axisymmetric gaseous fuel jet in air show a laminar behaviour up to  $Re=w_0D_0/\nu < 1000$ , with a flame height increasing linearly with exit velocity (see Flame length). A transition to turbulent jet combustion takes place at higher  $Re$  (up to  $Re > 2000$  for  $H_2$  but  $Re > 9000$  for  $C_3H_8$ ), with a fully-turbulent flame-length independent of speed for higher Reynolds numbers. For instance, for a methane/air jet issuing from an orifice 1 mm in diameter, laminar flames are obtained for injection speeds up to 20 m/s, and turbulent flames up to 40 m/s, beyond which the flame detaches from the rim of the injector but remains stabilised in a lifted position (increasing with flow-rate to more than 10 diameters) up to 80 m/s, when it blows-off and extinguishes. Larger diameter flames do not blow off, explaining why natural-gas and oil-well fires cannot be extinguished by blowing out.

### Turbulent premixed flames

Laminar premixed flames were characterised by a propagation speed that only depended on fluid properties (fuel and oxidiser type, concentrations, temperature and pressure). Turbulent premixed flame speed, however, is dominated by turbulence intensity. For low turbulence-intensity levels, the flame appears wrinkled in many connected flamelets along the main flame front. For larger turbulence-intensity levels, the flamelets get disconnected, being transported by the eddies, until a generalised bulk reaction zone develops.

## CHEMICAL KINETICS

Thermochemistry considers how much heat, work and temperature can be obtained from a combustion reaction, and how is the exhaust composition, but says nothing about the reaction rate, i.e. how quick the process takes place, what is key to define the size of combustors.

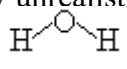
The interest now is in the reaction rate,  $\dot{\xi}$ , for a given reaction (or better its density  $\dot{\xi}/V$ , to have an intensive variable), instead of the reaction advance at equilibrium,  $\xi_{eq}$ , as in Thermochemistry. Recalling:

$$\xi \equiv \frac{n_i - n_{i0}}{\nu_i}, \quad \dot{\xi} = \frac{d\xi}{dt}, \quad \frac{\dot{\xi}}{V} = \frac{dn_i}{V\nu_i dt} = \frac{dc_i}{\nu_i dt}, \quad \text{for a given reaction } 0 = \sum \nu_i M_i \quad (51)$$

where  $c_i$  is the molar concentration of species  $i$  in the mixture (the common units used being mol per litre, mol/L, and the SI unit mol/m<sup>3</sup>).

But before specific kinetic models can be developed to study basic combustion processes, a review of general chemical kinetics is due.

### REACTION MECHANISM AND REACTION RATE

Consider the reaction of hydrogen with oxygen to yield water, that we usually write as  $\text{H}_2 + (1/2)\text{O}_2 = \text{H}_2\text{O}$ , and let us think at the molecular level of detail. First, we should write  $2\text{H}_2 + \text{O}_2 = 2\text{H}_2\text{O}$  because you can have half-a-mole, but not half-a-molecule. Second, we should write  $2\text{H}_2 + \text{O}_2 \rightarrow 2\text{H}_2\text{O}$  because we focus the attention on the forward reaction and not on the backward one (i.e. the possible decomposition of water to hydrogen and oxygen). But third, it is clearly unrealistic to think that in a single step two H-H molecules interact with one O=O molecule to yield two  molecules.

Instead of the above global reaction, a more realistic elementary mechanism must be thought of in terms of uni-molecular, bimolecular and ter-molecular steps.

- Uni-molecular reactions are those where one molecule of reactive breaks down by collision with an unspecified molecule at a very high relative speed, or when an already excited molecule hits another and decompose. The unspecified molecule is required to balance the momentum and energy of the uni-molecular chemical change. Example: the combustion of hydrogen must start by dissociation of a hydrogen molecule (it requires less energy than oxygen dissociation):  $\text{H}_2 + \text{M} \rightarrow \text{H} + \text{H} + \text{M}$ , where M stands for an unspecified molecule (hydrogen, oxygen, a hot wire). Uni-molecular reactions are very rare at low temperature (the fraction of molecules with very large speeds according to the Maxwell-Boltzmann distribution law is not enough to flame the system and propagate the reaction, except when locally excited (e.g. spark ignition) or globally heated (autoignition)).
- Bimolecular reactions are those where two molecules of reactives recombine by collision because of their very high relative speed or because they are already excited; example in the combustion of hydrogen may be  $\text{H}_2 + \text{O}_2 \rightarrow \text{HO}_2 + \text{H}$  and  $\text{H}_2 + \text{OH} \rightarrow \text{H}_2\text{O} + \text{H}$ , respectively.
- Ter-molecular reactions are those where three molecules happen to collide together at the same time. Ter-molecular collisions are very much improbable than bimolecular collisions, but they are

more fertile (a larger fraction of chocks yield chemical change) because there are more possibilities for the redistribution of momentum and energy. An example in the combustion of hydrogen may be  $\text{H}+\text{OH}+\text{M}\rightarrow\text{H}_2\text{O}+\text{M}$ .

The many intermediate species appearing (e.g. H, HO<sub>2</sub>, OH,...) are called radicals (e.g. atomic hydrogen radical, hydroperoxide radical, hydroxyl radical,...); they are electrically neutral but with unpaired electrons. For instance, in the combustion of hydrogen in oxygen, a reaction mechanism with some 40 elementary reactions involving 8 species (H<sub>2</sub>, O<sub>2</sub>, H<sub>2</sub>O, OH, O, H, H<sub>2</sub>O and H<sub>2</sub>O<sub>2</sub>) has been found appropriate to model the real reaction in an ample temperature and pressure range. For the combustion of methane in air, current successful models use nearly 300 elementary reactions involving some 50 species. Most of the times, a reaction mechanism is dependent on the range of temperatures and pressures involved, and different mechanisms have to be developed for free-flame kinetics, for ignition kinetics, for very-low-pressure kinetics (wall effects become predominant), for porous burning kinetics, etc.

But for either the global reaction or any elementary reaction in a reaction mechanism, the question remains: what are the parameters that influence the rate of advance? It was well-known that increasing temperature had a tremendous influence on the reaction rate; for the influence of pressure there was little knowledge and little interest; but how about the influence of the reactives themselves? The answer is the law of mass action.

### Mass action law

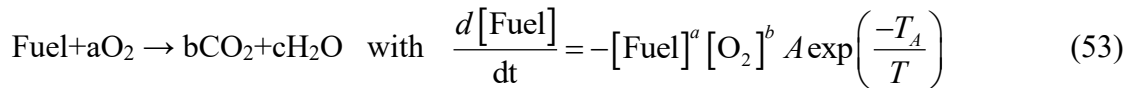
The Norwegian chemistry professors Cato Guldberg and Peter Waage (brothers in law), first presented in 1864, in their “Studies Concerning Affinity”, what they called ‘the action of masses in chemical reactions’, now called the law of mass action: “at a constant temperature and pressure, the rate of chemical reaction is directly proportional to the concentration of the reacting substances raised to particular exponents”. For instance, for the combustion of hydrogen in oxygen at some temperature and pressure, it is found:

$$\frac{\dot{\xi}}{V} = \frac{d[\text{H}_2\text{O}]}{2dt} = \frac{-d[\text{H}_2]}{2dt} = \frac{-d[\text{O}_2]}{dt} = k(T, p)[\text{H}_2]^{1.5}[\text{O}_2]^{0.7} \quad \text{for } 2\text{H}_2+\text{O}_2\rightarrow 2\text{H}_2\text{O} \quad (52)$$

where the common notation for concentrations  $[\text{M}]\equiv c_M$  has been used. The coefficient  $k(T, p)$  is called ‘rate coefficient’. The sum of the exponents is called ‘reaction order’ (order 2.2 (1.5+0.7) in the example), and each exponent is called ‘reaction order in that species’ (1.5 order in H<sub>2</sub> and 0.7 order in O<sub>2</sub>).

Theoretical kinetic models have been developed for practical combustion processes, basically for combustion of hydrogen and of methane, but the mechanism is very complex, with tens of elementary species and hundreds of elementary reactions. For hydrocarbons, the two controlling steps seem to be the formation of molecular hydrogen from hydrogen radicals (e.g.  $\text{CH}_4+\text{H}=\text{CH}_3+\text{H}_2$ ) and the consumption of molecular oxygen by combination with hydrogen radicals ( $\text{H}+\text{O}_2=\text{HO}_2$ ).

Empirical reaction rates for hydrocarbons have been developed based on the simplification that the fuel (with the oxidiser) first oxidises to CO and H<sub>2</sub>O, and in a second step CO further oxidises to CO<sub>2</sub> (for lean mixtures), and even for the global complete combustion to CO<sub>2</sub> and H<sub>2</sub>O:



Where a, b and c are the stoichiometric coefficients, and a, b, A and T<sub>A</sub> are empirical coefficients whose values are given in Table 3.

Table 3. Empirical coefficients in Eq. (53) for the global combustion reaction of some hydrocarbons (units for A, a and b compatible with concentrations in mol/m<sup>3</sup>).

Fuel	A	a	b	T <sub>A</sub>
Methane	83 · 10 <sup>9</sup>	-0.3	1.3	15 000 K
Propane	27 · 10 <sup>6</sup>	0.1	1.65	15 000 K
Butane	23 · 10 <sup>6</sup>	0.15	1.6	15 000 K
n-Octane	15 · 10 <sup>6</sup>	0.25	1.5	15 000 K
Methanol	10 · 10 <sup>6</sup>	0.25	1.5	15 000 K

But the real importance of the law of mass actions comes when applied to elementary reactions, since then the reaction order is just the number of molecules participating. For instance, for H+O<sub>2</sub>→OH+O the reaction speed density is d[OH]/dt=k[H][O<sub>2</sub>]. For a generic elementary reaction aA+bB=Products, the law of mass action is then:

$$\frac{\dot{\xi}}{V} = \frac{-dc_A}{adt} = \frac{-dc_B}{bdt} = k(T, p) c_A^a c_B^b \quad \text{for } aA + bB \rightarrow P \quad (54)$$

### Types of elementary reactions

According to their reaction order, the main type of reactions are first, second and third order reactions.

- First order reactions serve to model decomposition reactions A+M→B+M when the concentration of the unspecified molecule M is much larger than the reactive species A. The concentration of the active species varies exponentially with time, d[A]/dt=k[A], and the rate coefficient can be computed from two concentration measurements (at two instants). It was Lindemann in 1922 who first explained the reaction mechanism for uni-molecular decompositions.
- Second order reactions serve to model the majority of elementary reactions (formation of activated complex, isomerisation, double decomposition) since bimolecular reactions are the most common.
- Third order reactions serve to model ter-molecular reactions. Ter-molecular collisions, although not as probable as bimolecular collisions, are much more fertile and thus many third-order reactions appear in reaction mechanisms. The common instance is the recombination of two active radicals after collision with a third body that absorbs energy, e.g. H+H+M→H<sub>2</sub>+M (without it, simple collisions between two active radicals are not productive).

According to their effect, the main types of elementary reactions are:

- Chain initiation and chain termination reactions. Initiation steps generate radicals from stable molecules (but they are very rare), and termination steps consume radicals yielding the end products (they are also very rare). Examples:  $\text{H}_2 + \text{M} \rightarrow \text{H} + \text{H} + \text{M}$  is an initiation reaction in hydrogen decomposition, and  $\text{OH} + \text{H} + \text{M} \rightarrow \text{H}_2\text{O} + \text{M}$  is a termination reaction in water formation. Combustion reactions generally start with the generic initiation step  $\text{RH} + \text{O}_2 = \text{R} + \text{HO}_2$ , where R is a hydrocarbon radical (e.g.  $\text{CH}_4 + \text{O}_2 = \text{CH}_3 + \text{HO}_2$ ).
- Chain propagation reactions are the majority in a reaction mechanism. Propagation steps produce new radicals by consuming other radicals (in the same amount, see below). Example:  $\text{H}_2 + \text{OH} \rightarrow \text{H}_2\text{O} + \text{H}$ .
- Chain branching occurs when one radical yields more than one radical upon collision with a stable molecule. Example:  $\text{O} + \text{H}_2 \rightarrow \text{OH} + \text{H}$ . It is this branching effect that characterises what are known shortly as ‘chain reactions’; reactions that become more and more productive because more and more active radicals are generated, causing an exponential growth rate termed ‘explosive’, only limited by the total amount of initial reactives. Combustion is the traditional example of chain reaction (also nuclear fission).

In order to render amenable the solution of the mathematical problem for the reaction mechanism, several simplifications are introduced, the most common being the steady state, the frozen equilibrium, the partial equilibrium, and the high activation energy.

- The steady state approximation is the assumption that very active radicals form and decompose at the same (high) rate, with negligible accumulation in the system. This reduces a differential equation to an algebraic one. For instance, in the Zeldovich mechanism of NO formation ( $\text{O} + \text{N}_2 \leftrightarrow \text{NO} + \text{N}$  and  $\text{N} + \text{O}_2 \leftrightarrow \text{NO} + \text{O}$ ) this approximation implies  $d[\text{N}]/dt = k_1[\text{O}][\text{N}_2] - k_2[\text{N}][\text{O}_2] = 0$ .
- The frozen equilibrium approximation is the assumption that slow rate reactions can be solved after faster reactions are solved, the former being sensitive only to the integral effect of the quicker processes. This eliminates a differential equation.
- The partial equilibrium approximation is applied when there are two species linked by a single fast reaction in both senses (forward and backward); then, the concentration of one of them can be simply put as proportional to the other through the equilibrium constant for that equation (forward and backward). This reduces a differential equation to an algebraic one.

### Arrhenius law

Once the effect of the concentration of reactives has been singled out with the law of mass action, the rate constant in (32) will depend on temperature, pressure and other side effects, as the presence of catalysts, or the type of solvent for liquid-phase reactions. The effect of pressure is negligible in condensed-phase reactions, and for gaseous reactions is already taken into account through the concentration of species, at least in the ideal gas model. But the effect of temperature is very great, with reaction rates doubling just by increasing temperature a few tens degrees. Well, most chemical reactions accelerate when increasing temperature, but there are some exceptions, notably in catalytically-controlled biological systems (i.e. with enzymes), where first the reaction rate increases but then decreases with further temperature rise.

Svante Arrhenius proposed in 1889 a dependence of rate coefficients with temperature, based on the integration of the theoretical deduction by van't Hoff in 1884 of his famous equation for the variation of the equilibrium reaction constant,  $K$ , with temperature (see e.g. [Thermodynamics of Chemical Reactions](#)):

$$\frac{d \ln K}{d \frac{1}{T}} = \frac{-h_r^\oplus}{R} \quad (55)$$

where  $h_r^\oplus$  is the standard reaction enthalpy and  $R$  the gas constant. Arrhenius proposed:

$$k(T) = Ae^{\frac{-E_a}{RT}} \quad (56)$$

and gave to  $E_A$  the interpretation of an energy barrier that the molecules have to jump over, to actually react; thence  $E_A$  is termed 'activation energy', and it is much larger than the denominator in (56) for combustion reactions. Coefficient  $A$  in (42) is known as the pre-exponential factor or the collision factor, since it can be calculated from collision theory, as shown below. Another variable, named activation temperature,  $T_A$ , is introduced instead of the activation energy as  $T_A \equiv E_A/R$ , with values of order  $10^4$  K for combustion reactions (Table 3).

The Arrhenius exponential temperature dependence, was deduced from van't Hoff equation for equilibrium, but it can be deduced also from collision theory assuming that the probability of a fertile chock is proportional to the number of molecules with kinetic energy above a threshold (the activation energy). In effect, Maxwell-Boltzmann distribution of molecular kinetic energies shows that the fraction of the total number of molecules,  $f$ , with normalised kinetic energy between  $\varepsilon$  and  $\varepsilon+d\varepsilon$  ( $\varepsilon$  is the kinetic energy divided by the mean kinetic energy), and its integral from  $\varepsilon$  to  $\infty$  are (Fig. 14):

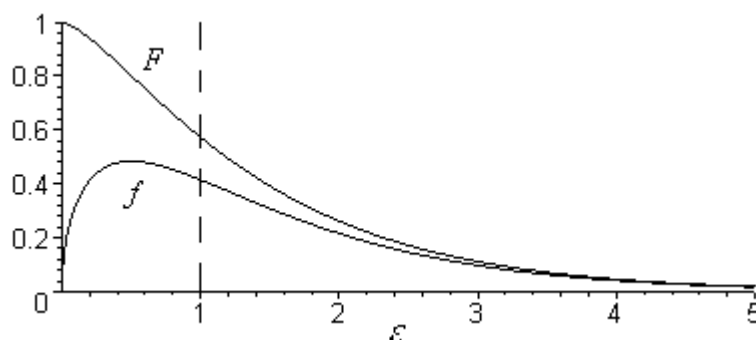


Fig. 14. Maxwell-Boltzmann distribution,  $f$ , of molecular kinetic energies (relative to the mean kinetic energy), and its integral from  $\varepsilon$  to  $\infty$ ,  $F$ .

$$fd\varepsilon = \frac{2}{\sqrt{\pi}} \sqrt{\varepsilon} e^{-\varepsilon} d\varepsilon \rightarrow F(\varepsilon) = \int_{\varepsilon}^{\infty} fd\varepsilon = 1 - \operatorname{erf}(\sqrt{\varepsilon}) + \frac{2}{\sqrt{\pi}} \sqrt{\varepsilon} e^{-\varepsilon} \stackrel{\varepsilon \gg 1}{\approx} \frac{2}{\sqrt{\pi}} \sqrt{\varepsilon} e^{-\varepsilon} \quad \text{with} \quad \varepsilon \equiv \frac{\frac{1}{2}mv^2}{\frac{3}{2}kT} \quad (57)$$

where  $m$  is the mass of a molecule,  $v$  the modulus of its velocity, and  $k$  Boltzmann's constant (the gas constant divided by Avogadro's number,  $k=R/N_A$ ). That is, the fraction of molecules with kinetic energies larger than a given value is proportional to an exponential factor in temperature of the form  $\exp(-1/T)$ . Notice that there is  $-1/T$  and not  $T$  in the exponential argument in (56), contrary to what might be thought by saying that reaction rates grow exponentially with  $T$  (in fact, the Arrhenius exponential factor tends to 1 for large temperatures, not to infinity). One may recover the reasoning in terms of temperature variations,  $\Delta T$ , relative to a given value,  $T_0$ , and expanding  $\exp(-T_A/(T_0+\Delta T)) \propto \exp(\Delta T)$ . The molecular kinetic-energy distribution also shows a  $T^{-1/2}$  pre-exponential temperature-dependence (the  $\sqrt{\varepsilon}$  term), but it does not correspond well to experimental data, and an empirical exponent,  $T^a$ , is sometimes used instead.

### Collision theory

Collision theory for bimolecular reactions gives a simple explanation to both the mass action law and Arrhenius law. The argument is as follows. The reaction rate density should be proportional to the number of collisions per unit volume and unit time, multiplied by the probability that a collision be fertile (i.e. that produces new species; most collisions are sterile in the sense that only yield thermal redistribution of energy, i.e. changes in translational, rotational or vibrational energies, without chemical change, i.e. changes in electronic configuration).

The number of collisions per unit volume, for a molecule A with molecules B (assume there are type A and type B molecules only), can be estimated roughly as the number of intersecting points (molecules centres) in a cylindrical volume of length  $\bar{v}dt$  and diameter double than the average molecule diameter (double because only their centre points were considered before); i.e.:

$$\left( \frac{\text{number of collisions for one molecule}}{\text{unit volume} \square \text{unit time}} \right) = \frac{N_B}{V} \bar{v} \frac{\pi(2\sigma)^2}{4} \quad (58)$$

where  $N_B/V$  is the number of B-molecules per unit volume (its molar concentration,  $c_B$ , times Avogadro's number), and  $\sigma$  is the averaged diameter of the molecules. When all molecules are considered for the number of bimolecular collisions, and substituting the characteristic speed,  $\bar{v}$ , according to the Maxwell-Boltzmann distribution, the final result is:

$$\left( \frac{\text{number of total collisions}}{\text{unit volume} \square \text{unit time}} \right) = c_A c_B \sqrt{\frac{8k_B T}{\pi \mu_{AB}}} \pi \sigma^2 \quad (59)$$

On the other hand, the probability that a collision be fertile must be proportional to the fraction of molecules with a high-enough speed (the tail of the Maxwell-Boltzmann distribution, Fig. 14), and to some steric factor that accounts for the fact that, for the same high speed, the geometry of the multi-atom molecules on the collision must be important to fertility (e.g. *ceteris paribus*, the fertility of the OH+H collision to yield H<sub>2</sub>O must depend on the orientation of the linear OH-radical relative to the centre of the H radical (chocks where the O-atom lies in the middle will be more productive). Considering just the tail

of the Maxwell-Boltzmann distribution, it is proportional to the exponential of the chosen lower energy bound (43), i.e.:

$$\left( \begin{array}{l} \text{probability that a} \\ \text{collision is fertile} \end{array} \right) \propto \exp\left(\frac{-E_A}{RT}\right) \quad (60)$$

where  $E_A$  is the activation energy for the reaction (for the reaction  $A+B \rightarrow P$ ; not just to species A). In summary:

$$\frac{\dot{\xi}}{V} = \frac{-dc_A}{dt} = \frac{-dc_B}{dt} = c_A c_B A \left(\frac{T}{K}\right)^b \exp\left(\frac{-E_A}{RT}\right) \quad (61)$$

where  $A$  is the pre-exponential factor as in Arrhenius law, and  $K$  stands for the temperature unit, the kelvin, to have a non-dimensional exponent  $b$  (the  $K$  is omitted in most writings). For real work, the three parameters  $A$ ,  $b$  and  $E_A$  are experimentally determined because the collision theory do not provide any values for them, although a more refined activated-complex theory (with bonding energies and steric factors) could be developed to supply estimations of those parameters in terms of more basic data.

Activation energy data are given in MJ/mol units (usually written as kJ/gmol), or as activation temperatures,  $T_A = E_A/R$  in kelvin units. Exponent  $b$  is tabulated in non-dimensional form, as said above, in spite of the fact that most of the times  $T^b$  is written in (61) instead of  $(T/K)^b$ . Finally,  $B$  is commonly given in CGS-units of  $(\text{cm}^3/\text{gmol})^{n-1}/\text{s}$ , where  $n$  is the reaction order, instead of the SI-units  $(\text{m}^3/\text{mol})^{n-1}/\text{s}$ . Table 4 gives a sample of experimental values.

Table 4. Empirical values in Eq. (61) for some elementary reactions in the combustion of hydrogen with oxygen (from Warnatz-1984).

Reaction	$A$	$b$	$E_A$	Temperature range
$\text{H} + \text{O}_2 \rightarrow \text{OH} + \text{O}$	$1.2 \cdot 10^{17} (\text{cm}^3/\text{gmol})/\text{s}$	-0.91	69.1 MJ/mol	300..2500 K
$\text{O} + \text{H}_2 \rightarrow \text{OH} + \text{H}$	$1.5 \cdot 10^7 (\text{cm}^3/\text{gmol})/\text{s}$	2.0	31.6 MJ/mol	300..2500 K
$\text{H} + \text{OH} + \text{H}_2\text{O} \rightarrow 2\text{H}_2\text{O}$	$1.4 \cdot 10^{23} (\text{cm}^3/\text{gmol})^2/\text{s}$	-2.0	0	1000..3000 K
$\text{H}_2\text{O} + \text{H}_2\text{O} \rightarrow \text{H} + \text{OH} + \text{H}_2\text{O}$	$1.6 \cdot 10^{17} (\text{cm}^3/\text{gmol})/\text{s}$	0	478 MJ/mol	2000..5000 K

### Relation between rate coefficients and equilibrium constants

Global reactions indicate overall transformations, with a clear distinction between starting reactives and end products, i.e. there is an assumed direction of advance. Elementary reactions, however, indicate detailed interactions that, in principle, can be assumed to have no privileged direction of advance, i.e. they should be at equilibrium (generating products at the same rate as they react back). For a reaction at equilibrium, the quotient of rate coefficients (forward/backward) must equal the equilibrium constant. In effect, applying Eq. (52) to both senses of a generic reaction  $aA + bB \leftrightarrow cC + dD$ , one gets:

$$\left. \begin{aligned} \frac{\xi_f}{V} &= k_f(T, p) c_A^a c_B^b \\ \frac{\xi_b}{V} &= k_b(T, p) c_C^c c_D^d \end{aligned} \right\} \xi_f = \xi_b \Rightarrow \frac{k_f(T, p)}{k_b(T, p)} = \frac{c_C^c c_D^d}{c_A^a c_B^b} = K_c(T, p) = K(T, p^\oplus) \left( \frac{p^\oplus}{RT} \right)^{c+d-a-b} \quad (62)$$

Measurement of rate coefficient is so difficult that it is usual to get just one significant figure in accuracy, so that even far from equilibrium, the relation between rate coefficients at equilibrium and the equilibrium constant is used to evaluate either the backward or the forward rate coefficient, based on the measurement of the other.

Several kinetic mechanisms have been worked out of combustion interest. Some of them are very simple, as the one step kinetics for ozone formation (O<sub>2</sub>/O<sub>3</sub>/O kinetics), other are relatively simple, as the burning of hydrogen with halogens or the formation of nitrogen oxides, but typical combustion processes are really entangled; a short-mechanism for CH<sub>4</sub>/air combustion already involves 14 species: CH<sub>4</sub>, O<sub>2</sub>, N<sub>2</sub>, CO<sub>2</sub>, H<sub>2</sub>O, CO, H<sub>2</sub>, OH, H, O, OH<sub>2</sub>, CH<sub>3</sub>, HCHO and CHO. In the case of a lean combustion, the oxidation pattern seems to be CH<sub>4</sub>→CH<sub>3</sub>→HCHO→HCO→CO→CO<sub>2</sub>.

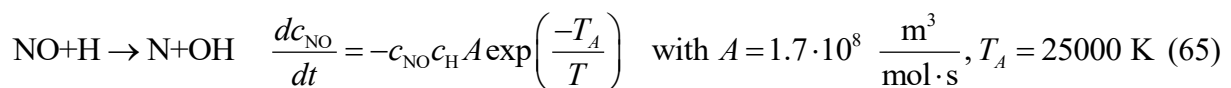
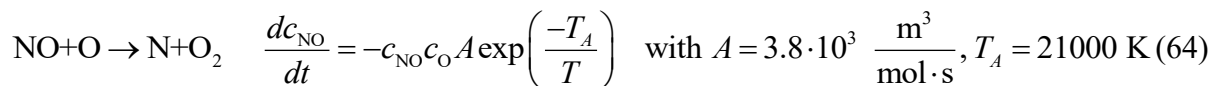
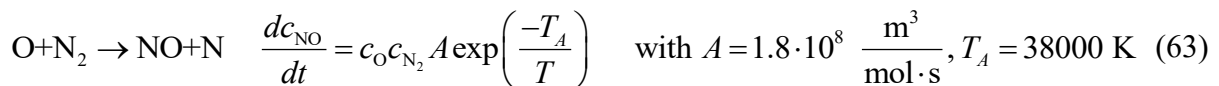
To simplify the kinetic mechanism, two basic assumptions are often introduced, the steady state and the partial equilibrium hypothesis:

- Some radicals are assumed to be produced and consumed at a steady rate (not valid at the start and the end of the process)
- Some elementary reactions are assumed to be so quick that they are at equilibrium (forward rate equal to backward rate) at the time scale considered.

## KINETICS OF NO<sub>x</sub> FORMATION

Chemical kinetics has not yet been able to provide accurate models for practical combustion reactions, but has proved invaluable to understand some basic associated processes, particularly the formation of emissions. The best known example is the Zeldovich-kinetics mechanism for NO<sub>x</sub> formation.

Normal combustion in air produces some 1000..4000 ppm of NO and some 10..40 ppm of NO<sub>2</sub>. Although NO<sub>x</sub> formation may come from a N-containing fuel, from reaction of N<sub>2</sub> in air within the flame front, or from reaction in the hot-products region, for lean adiabatic combustion it is the latter, the thermal formation after the flame, that is dominant. The extended Zeldovich mechanism is:



the last reaction being added to the basic Zeldovich mechanism to better model near-stoichiometric combustion cases. The rate of NO formation is computed from:

$$\frac{dc_{\text{NO}}}{dt} = k_1 c_{\text{O}} c_{\text{N}_2} - \frac{k_1}{K_1} c_{\text{NO}} c_{\text{N}} - k_2 c_{\text{NO}} c_{\text{O}} + \frac{k_2}{K_2} c_{\text{N}} c_{\text{N}_2} - k_3 c_{\text{NO}} c_{\text{H}} + \frac{k_3}{K_3} c_{\text{N}} c_{\text{OH}} \quad (66)$$

with  $k_1$ ,  $k_2$  and  $k_3$  being the rate coefficients for the three reactions above,  $K_1$ ,  $K_1$  and  $K_1$  being their equilibrium constants, and  $c_{\text{O}}$ ,  $c_{\text{N}_2}$ ,  $c_{\text{N}}$ ,  $c_{\text{O}_2}$  and  $c_{\text{OH}}$  corresponding to the equilibrium exhaust composition in absence of NO.

## CATALYSIS

A catalyst is a substance that changes the velocity of a chemical reaction while not being changed itself overall, and may be highly selective in their activity, as shown for instance by their effect on ethyl alcohol, which is stable at ambient temperature; in the presence of an alumina catalyst, ethyl alcohol will react to form diethyl ether or ethylene, and, if the alumina is replaced by copper, the products become acetaldehyde and hydrogen. It should be emphasized that a catalyst only speeds up the rate of a reaction that is thermodynamically allowed, even if its rate is so small as to be negligible. A platinum catalyst will initiate and accelerate the reaction of hydrogen and oxygen to form water, but no catalyst will facilitate the reverse reaction, the decomposition of water into hydrogen and oxygen at room temperature. The latter reaction is not allowed by thermodynamics to run alone.

Catalysts are usually classified as:

- Homogeneous catalysts. Of little relevance in combustion. They are often coordination compounds of transition metals soluble in the liquid medium in which the reaction takes place.
- Heterogeneous catalysts. They are finely divided solids (metals, metal oxides, metal sulphides, or acidic oxides) that catalyze reactions in a fluid media. Metal catalysts are usually transition metals such as iron, which catalyzes the synthesis of ammonia; platinum, which catalyzes the oxidation of hydrogen to water and of ammonia to nitric acid; platinum on alumina, which catalyzes the reforming of petroleum to high-octane gasoline; molybdenum sulphide, which catalyzes removal of sulfur from crude petroleum; etc. Gasoline is processed by a catalytic reaction carried out over alumina silicates (zeolites).
- Enzymes. They are biological catalysts, complex organic compounds that contain a protein entity, and are the most active in Nature.

The combustion catalyst per excellence is platinum (Pt); the catalytic property of Pt were discovered by the German chemist J.W. Dobereiner in 1820 in the hydrogen/oxygen reaction to form water at room temperature. In 1887 the French pharmacist M. Berger patented the Berger lamp, a 'hygienic lamp and smoke absorber', that consists on an alcohol lamp (with secret essential-oil odorants), with a wick connected to a burner made up of ceramic and black platinum, that, when heated up for a couple of minutes, has the ability to retain a smokeless incandescence at some 500 °C (it was much used in mortuaries and hospitals, and nowadays in aromatherapy).

## The three-way catalytic converter

For unburnt emissions, the catalytic after-treatment of the exhaust gas is considerably more effective than the purely thermal after-burning of the exhaust gases in a thermal reactor. Using a modern catalytic converter, more than 90% of the amount of toxic substances can be converted to harmless substances.

The so called three-way catalytic converter (TWC, see Combustion Instrumentation), has come into widespread use for gasoline engines (on all new cars since 1993). The term "three-way" means that all three toxic substances CO, HC and NO<sub>x</sub> are eliminated at the same time, although there are really only two different processes: the oxidation of the unburnt emissions (CO and HC), and the reduction of the nitrogen oxides. The converter shell contains a ceramic "honeycomb" which is coated with a noble-metal combination (platinum, palladium and rhodium), although some other catalysts are being tried, as perovskite (a greyish-black mineral form of calcium titanate, with some rare-earth elements, which is used in certain high-temperature ceramic superconductors). Only lead-free gasoline may be used with noble-metal converters because the lead otherwise destroys the catalytic properties of the metals. The catalytic converter also works on natural-gas burning engines, but not for sewage and landfill biogases because sulfur and heavy metals content rapidly deactivate the catalyst.

The three-way catalytic converter only reduce NO<sub>x</sub> in rich mixtures and only oxidise CO and HC in lean mixtures, with a very thin overlapping region near the stoichiometric air-fuel ratio (a deviation of only 1 % has considerable adverse effects on either oxidation or reduction efficiency). That is why they are only useful for gasoline engines, and only if running stoichiometric. Moreover, the best open-loop engine-control would be unable to maintain the air-fuel mixture within the close tolerances required for optimum work of the three-way catalytic converter, and so an extremely accurate closed-loop electronic control (featuring almost zero lag), with an oxygen sensor at the exhaust (the lambda probe), must be added to the air-fuel-mixture management system.

## Selective catalytic reduction (SCR)

As the successful three-way catalytic converter only works close to stoichiometric mixing, other catalysts are being tried for lean-mixture gasoline and all diesel engines (always lean), specifically designed to get rid of the NO<sub>x</sub> since there is little CO and HC in lean-combustion engines.

For lean-mixture gasoline engines, CO and HC are oxidised with a platinum catalysts in a first-order reaction mechanism since only the CO or HC concentration is controlling, oxygen concentration being much higher in lean combustion products (e.g. for  $\text{CO} + (1/2)\text{O}_2 \rightarrow \text{CO}_2$ ,  $\dot{\xi}/V = k(T)x_{\text{CO}}$ ).

For diesel engines, best results (>90% NO<sub>x</sub> reduction) are presently obtained by spraying urea in the flue gases, to generate ammonia by thermo-hydrolysis  $(\text{NH}_2)_2\text{CO} + \text{heat} = \text{HNCO} + \text{NH}_3$  followed by hydrolysis of the isocyanic acid  $\text{HNCO} + \text{H}_2\text{O} + \text{heat} = \text{NH}_3 + \text{CO}_2$ , in a selective catalytic reduction (SCR) process through a platinum-coated titanium-oxide matrix. The urea aqueous solution (40%wt) is carried in a reservoir and fed by a dosing pump (the amount of urea depends on engine load) to a compressed-air spraying system. The urea SCR only works at  $T > 250$  °C, and it is found that near-equimolar NO/NO<sub>2</sub> mixtures proceed much faster than pure NO or NO<sub>2</sub>. In the first case the reaction is directly

$\text{NO} + \text{NO}_2 + 2\text{NH}_3 = 2\text{N}_2 + 3\text{H}_2\text{O}$ , whereas in the second case additional steps involving ammonium nitrate take place.

If the fuel contains sulfur (as some heavy fuel oils), there is the problem of condensation of  $(\text{NH}_4)_2\text{SO}_4$  downstream (that is why the SCR is placed after the exhaust turbine). Ethanol and other hydrocarbons have also been proved efficient for SCR, as well as other selective non-catalytic reducers (SNCR).

### **Catalytic combustion**

The usual thermal free-flame combustion process cannot be sustained in the vicinity (say within 1 mm) of normal cold solids (metals, ceramics or polymers), and thus it cannot propagate through normal cold porous media. But flames can propagate through hot porous solids and through cold porous solid-catalysts.

The catalytic substance helps to maintain the combustion process at low temperature at the surface, as when a mixture of  $\text{H}_2$ /air reacts over Pt at room temperature ( $\text{CH}_4$ /air over Pt requires  $350\text{ }^\circ\text{C}$ ), that in its absence would require much higher temperatures: the minimum autoignition temperature for homogeneous  $\text{H}_2$ /air combustion is 850 K

Catalytic combustion works for premixed flows and for a non-premixed fuel flow in ambient air, with steady temperatures in the catalytic matrix from 700 K to 1400 K. The advantages of power modulation, widening of ignition limits and less emissions, are similar to high-temperature porous combustion, or even better ( $<1$  ppm for  $\text{NO}_x$  and CO, due to very low temperatures involved), but not the higher burning rate (that was due to thermal conduction along the hot solid matrix, and thus only  $600\text{ kW/m}^2$  are achieved instead of the  $3000\text{ kW/m}^2$  of thermal porous-medium burners. At intermediate temperatures, an hybrid regime of catalytic-assisted thermal combustion may be developed, where both heterogeneous and homogeneous reactions take place, an interesting trade-off solution when the catalyst is too expensive and very little can be used (in full catalytic mode, if there is insufficient catalyst, part of the fuel slips to the exhaust (increasing pollution and expense), or even the whole fuel if the catalyst cools down and deactivates. The influence of the flowrates is important; for instance, if a thin porous solid is doped with a catalyst and a premixed methane/air stream is forced through, an exothermic oxidation of the fuel takes place if the temperature is  $>600\text{ K}$ , releasing much of the lower heating value, what causes the matrix to reach some 1500 K at the outer surface (the hotter) in a flameless regime with a power of up to  $500\text{ kW/m}^2$ ; but if more gases are fed, small flames detach from the outer surface and, at about  $1000\text{ kW/m}^2$ , a blue flame with some 1900 K forms immediately close to the outer surface, that only reaches now some 600 K.

[Back to Combustion](#)